Nuclear Josephson-like gamma-emission

G.Potel, E. Vigezzi , F.Barranco, and R.A. Broglia

Livermore Nat. Lab., USA

INFN, Milano, Italy

Univ. of Seville, Spain

Niels Bohr Institute, Copenhagen, Denmark

DREB 2022, Santiago de Compostela

- Overview

1. Two Nucleon Transfer Reactions as transient Josephson Junctions.

2. Nuclear Superfluidity (BCS): A fast revision.

3. Josephson Junctions (DC and AC): A revision.

4. The Legnaro's 116Sn+60Ni 2NT and 1NT data at different E_cm:

5. Gamma emission in 1NT and 2NT channels

6. Role of the the barrier thickness (w) and bias potential (V) in Josephson Junctions.

1. Two Nucleon Transfer Reactions as transient Josephson Junctions.

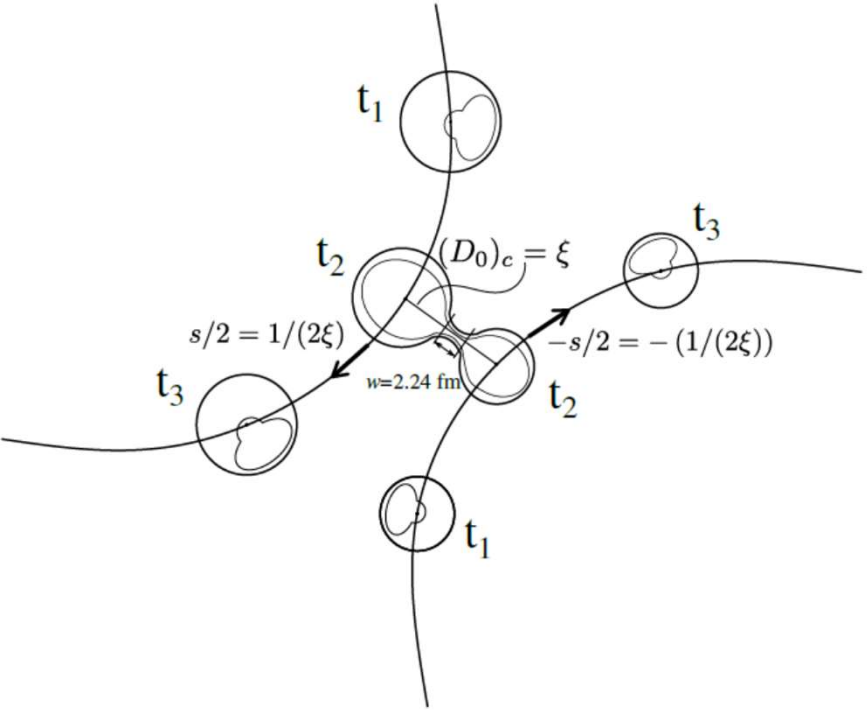

1. Two Nucleon Transfer Reactions as transient Josephson Junctions.

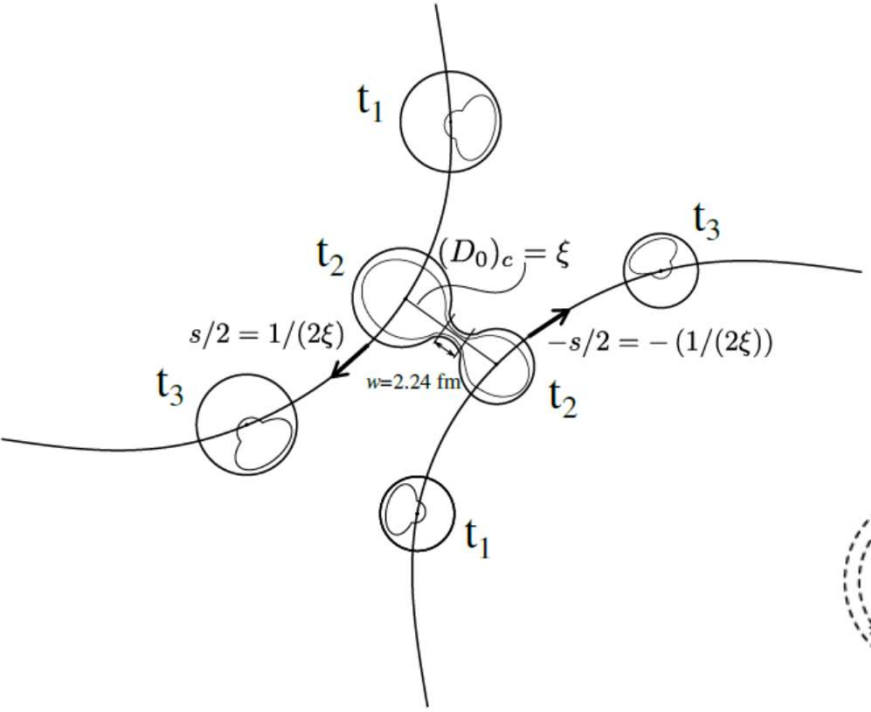

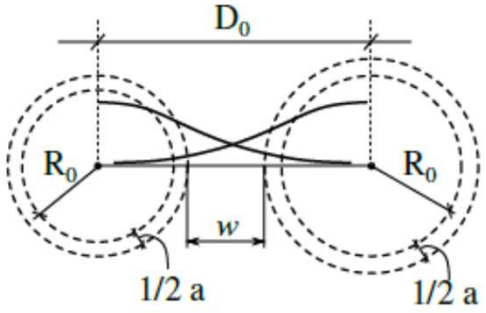

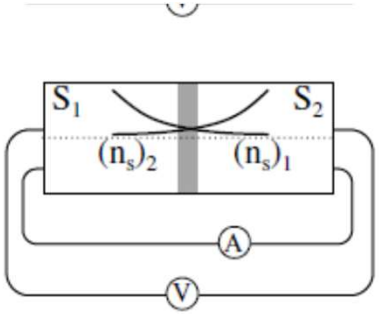

1. Two Nucleon Transfer Reactions as transient Josephson Junctions.

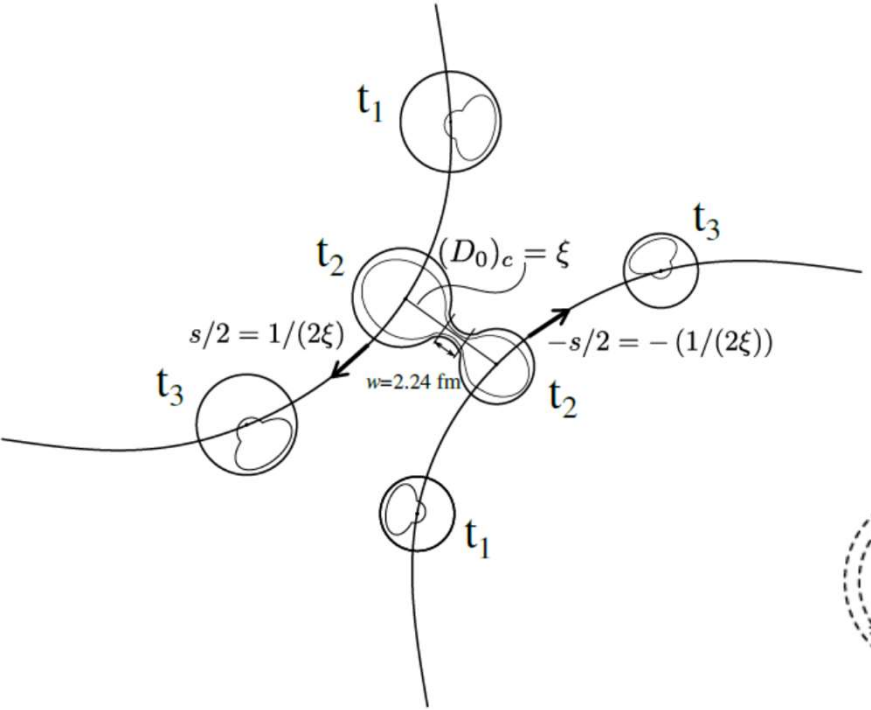

$$V_J^N = Q_{2n}/2e_{eff}$$

$$\omega_J = \frac{2eV_J^N}{\hbar} .= Q_{2n}/\hbar$$ Alternate current!!

The *Q*-value of the reaction acts as a "battery", providing an equivalent potential V^N.

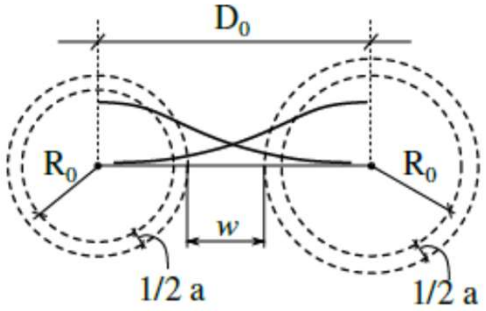

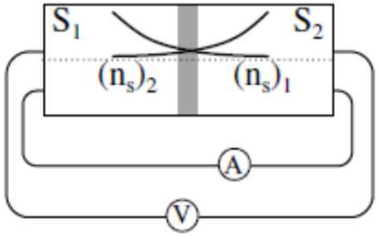

1. Two Nucleon Transfer Reactions as transient Josephson Junctions.

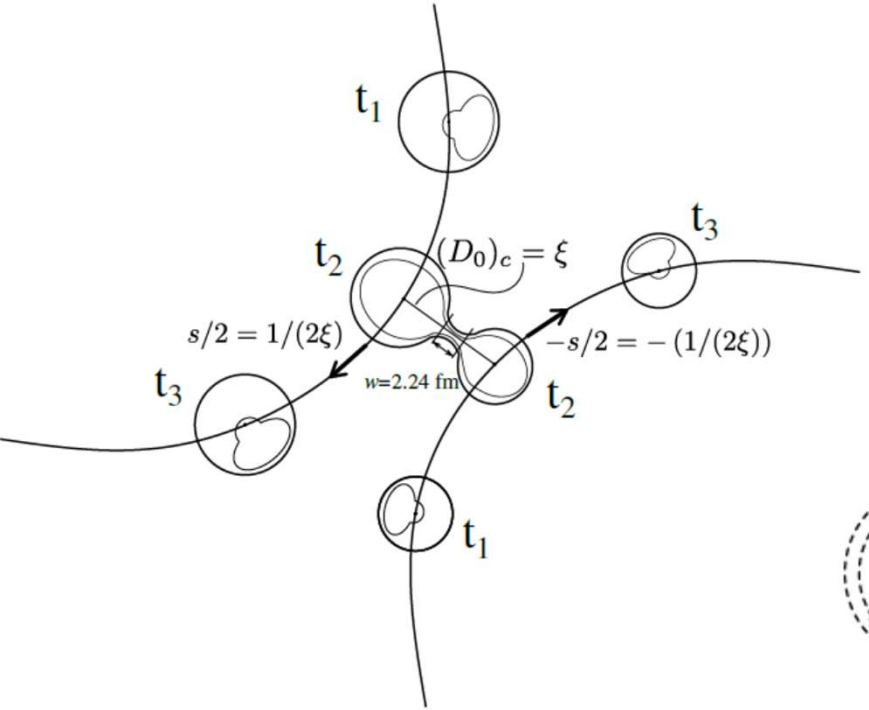

$$V_J^N = Q_{2n}/2e_{eff}$$

$$\omega_J = \frac{2eV_J^N}{\hbar} .= Q_{2n}/\hbar$$

Alternate current!!

The *Q*-value of the reaction acts as a "battery", providing an equivalent potential V^N.

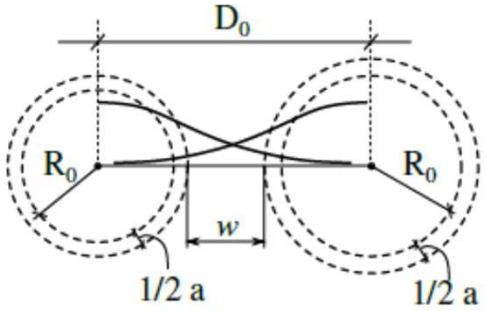

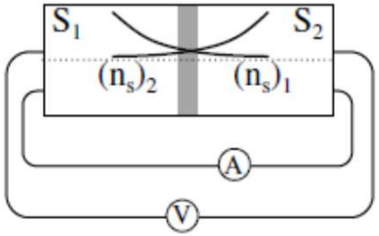

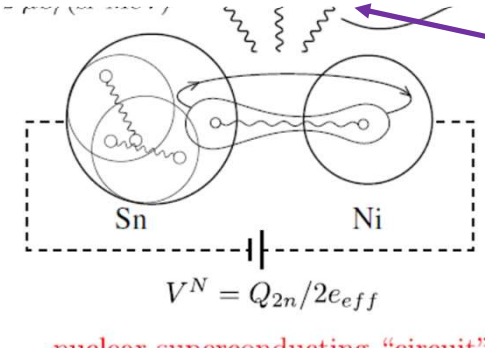

gamma's !!

2. Nuclear Superfluidity: The origin.

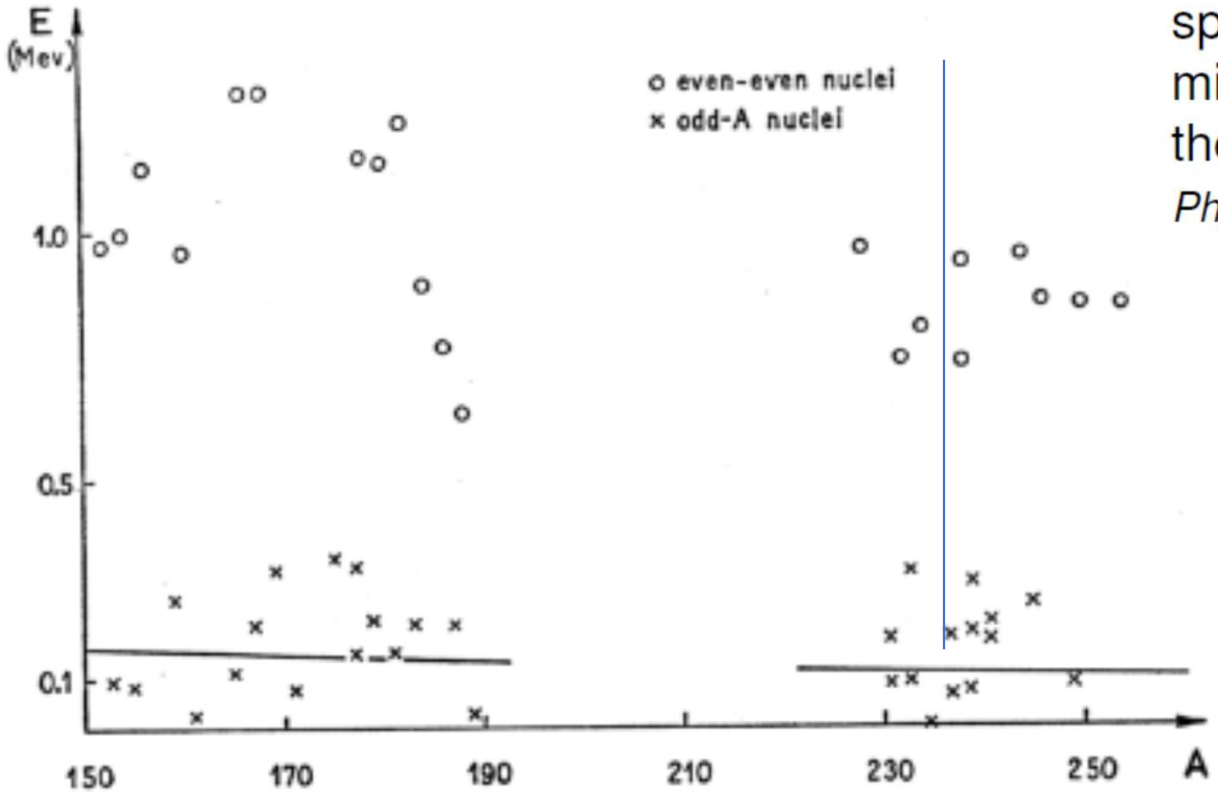

Bohr, Mottelson, and Pines speculated that nuclear pairing might explain the **energy gap** in the excitation spectra of nuclei.

Phys. Rev. 110, 936 (1958)

2. Nuclear superfluidity: BCS ground state

$$|BCS\rangle = \prod_k \left(U'_k + e^{-2i\phi} V'_k a^\dagger_{\mathbf{k+s},\uparrow} a^\dagger_{\mathbf{-k+s},\downarrow}\right)|0\rangle.$$

$$\begin{aligned}
\alpha^\dagger_\nu &= u_\nu a^\dagger_\nu - v_\nu a_{\bar\nu} & a^\dagger_\nu &= u_\nu \alpha^\dagger_\nu + v_\nu \alpha_{\bar\nu} \\
\alpha^\dagger_{\bar\nu} &= u_\nu a^\dagger_{\bar\nu} + v_\nu a_\nu & a^\dagger_{\bar\nu} &= u_\nu \alpha^\dagger_{\bar\nu} - v_\nu \alpha_\nu \\
\alpha_\nu &= u_\nu a_\nu - v_\nu a^\dagger_{\bar\nu} & a_\nu &= u_\nu \alpha_\nu + v_\nu \alpha^\dagger_{\bar\nu} \\
\alpha_{\bar\nu} &= u_\nu a_{\bar\nu} + v_\nu a^\dagger_\nu & a_{\bar\nu} &= u_\nu \alpha_{\bar\nu} - v_\nu \alpha^\dagger_\nu.
\end{aligned}$$

$$\begin{aligned}
H' &= H - \lambda n \\
&= \sum_{\nu>0} (\varepsilon^{(0)}_\nu - \lambda)(a^\dagger_\nu a_\nu + a^\dagger_{\bar\nu} a_{\bar\nu}) - G \sum_{\mu,\nu>0} a^\dagger_\mu a^\dagger_{\bar\mu} a_{\bar\nu} a_\nu,
\end{aligned}$$

$$\sum_{\nu>0} \left\{1 - \frac{\varepsilon_\nu - \lambda}{[(\varepsilon_\nu - \lambda)^2 + \Delta^2]^{\frac{1}{2}}}\right\} = N.$$

$$\frac{G}{2} \sum_{\nu>0} \frac{1}{[(\varepsilon_\nu - \lambda)^2 + \Delta^2]^{\frac{1}{2}}} = 1.$$

$$u^2_\nu = \frac{1}{2}\left\{1 + \frac{\varepsilon_\nu - \lambda}{[(\varepsilon_\nu - \lambda)^2 + \Delta^2]^{\frac{1}{2}}}\right\}$$

$$v^2_\nu = \frac{1}{2}\left\{1 - \frac{\varepsilon_\nu - \lambda}{[(\varepsilon_\nu - \lambda)^2 + \Delta^2]^{\frac{1}{2}}}\right\}.$$

2. Nuclear Superfluidity: Occupations.

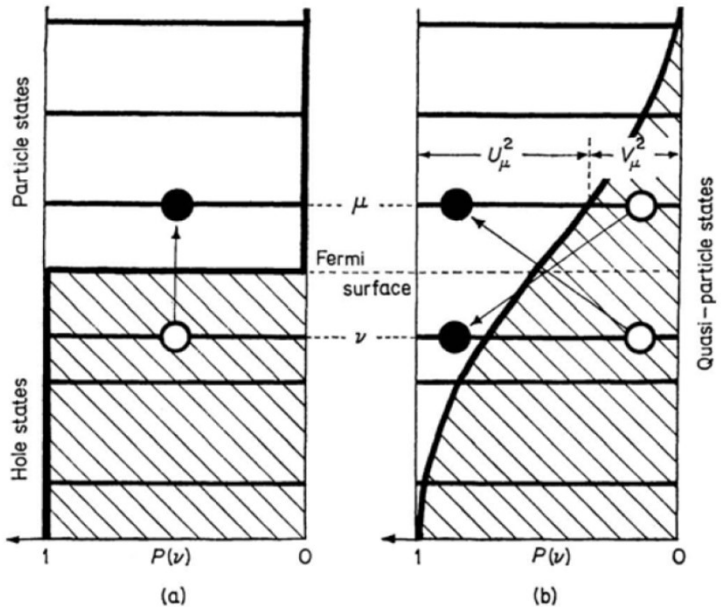

In figure 11.4 are shown experimental values of v_j^2 obtained by Cohen and Price (1961) from (d,p) and (d,t) experiments on the Sn

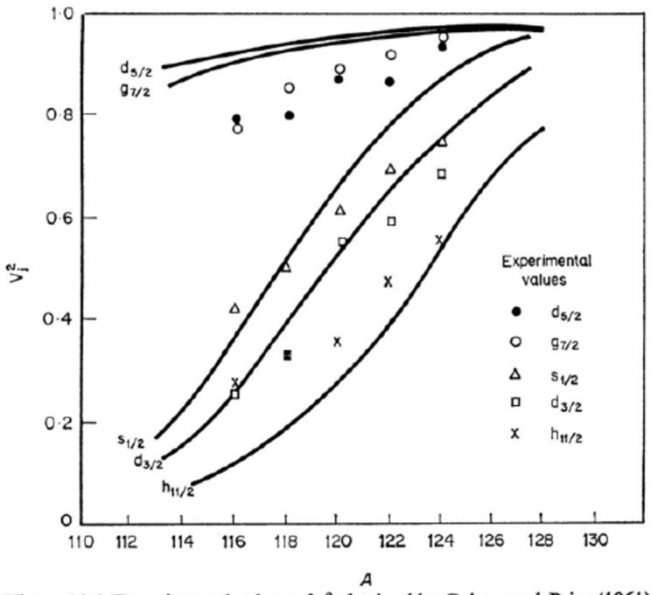

Figure 11.4. Experimental values of v_j^2 obtained by Cohen and Price (1961) from (d,p) and (d,t) experiments on the Sn isotopes, compared to the theoretical values of Kisslinger and Sorensen (1960).

D.Rowe, Nucl. Coll. Motion, Dover.

2. Nuclear Superfluidity: Sn(p,t): Occupations

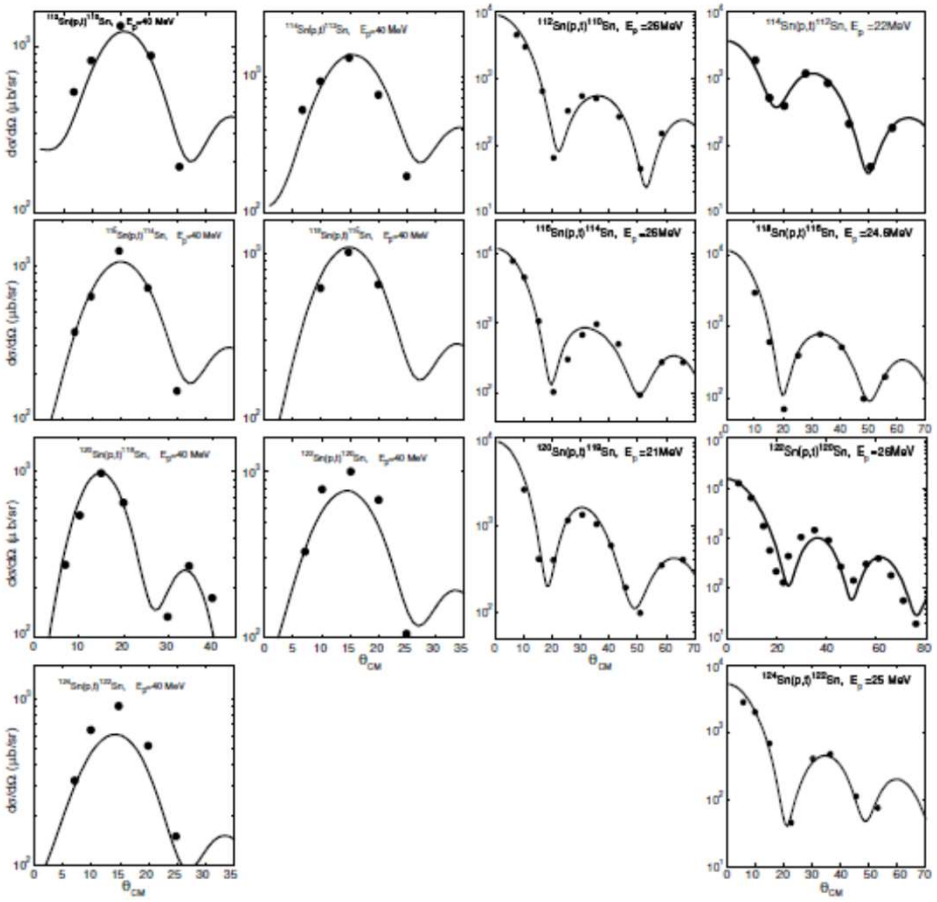

FIG. 7: Predicted absolute differential $^{A+2}\mathrm{Sn}(p,t)^{A}\mathrm{Sn}(gs)$ cross sections for bombarding energies 21 MeV $\leq E_p \leq$ 26 MeV, and E_p = 40 MeV in comparison with the experimental data (see [39–44] and [45] respectively).

Sn: 112 to 124

DWBA

$$\frac{d\sigma}{d\Omega} = \frac{\mu_i \mu_f}{(4\pi\hbar^2)^2}\frac{k_f}{k_i}\left|T^{(1)} + T^{(2)}_{succ} - T^{(2)}_{NO}\right|^2$$

$$T^{(1)} = 2\sum_{l_i,j_i}\sum_{\sigma_1\sigma_2}\int d\mathbf{r}_{tA}d\mathbf{r}_{p1}d\mathbf{r}_{A2}[\phi^{A+2}_{l_i,j_i}(\mathbf{r}_{A1},\sigma_1,\mathbf{r}_{A2},\sigma_2)]^{0*}_0\chi^{(-)*}_{pB}(\mathbf{r}_{pB})$$

$$\times v(\mathbf{r}_{p1})\phi_t(\mathbf{r}_{p1},\mathbf{r}_{p2})\chi^{(+)}_{tA}(\mathbf{r}_{tA}).$$

$$T^{(2)}_{succ} = 2\sum_{l_i,j_i}\sum_{l_f,j_f,m_f}\sum_{\substack{\sigma_1\sigma_2\\ \sigma'_1\sigma'_2}}\int d\mathbf{r}_{dF}d\mathbf{r}_{p1}d\mathbf{r}_{A2}[\phi^{A+2}_{l_i,j_i}(\mathbf{r}_{A1},\sigma_1,\mathbf{r}_{A2},\sigma_2)]^{0*}_0\chi^{(-)*}_{pB}(\mathbf{r}_{pB})v(\mathbf{r}_{p1})$$

$$\times\phi_d(\mathbf{r}_{p1})\varphi^{A+1}_{l_f,j_f,m_f}(\mathbf{r}_{A2})\int d\mathbf{r}'_{dF}d\mathbf{r}'_{p1}d\mathbf{r}'_{A2}G(\mathbf{r}_{dF},\mathbf{r}'_{dF})$$

$$\times\phi_d(\mathbf{r}'_{p1})^*\varphi^{A+1*}_{l_f,j_f,m_f}(\mathbf{r}'_{A2})\frac{2\mu_{dF}}{\hbar^2}v(\mathbf{r}'_{p2})\phi_d(\mathbf{r}'_{p1})\phi_d(\mathbf{r}'_{p2})\chi^{(+)}_{tA}(\mathbf{r}'_{tA})$$

$$T^{(2)}_{NO} = 2\sum_{l_i,j_i}\sum_{l_f,j_f,m_f}\sum_{\substack{\sigma_1\sigma_2\\ \sigma'_1\sigma'_2}}\int d\mathbf{r}_{dF}d\mathbf{r}_{p1}d\mathbf{r}_{A2}[\phi^{A+2}_{l_i,j_i}(\mathbf{r}_{A1},\sigma_1,\mathbf{r}_{A2},\sigma_2)]^{0*}_0\chi^{(-)*}_{pB}(\mathbf{r}_{pB})v(\mathbf{r}_{p1})$$

$$\times\phi_d(\mathbf{r}_{p1})\varphi^{A+1}_{l_f,j_f,m_f}(\mathbf{r}_{A2})\int d\mathbf{r}'_{p1}d\mathbf{r}'_{A2}d\mathbf{r}'_{dF}$$

$$\times\phi_d(\mathbf{r}'_{p1})^*\varphi^{A+1*}_{l_f,j_f,m_f}(\mathbf{r}'_{A2})\phi_d(\mathbf{r}'_{p1})\phi_d(\mathbf{r}'_{p2})\chi^{(+)}_{tA}(\mathbf{r}'_{tA})$$

Potel et al, Rep.Prog.Phys.76(2013)106301

2. Nuclear Superfluidity: Moments of Inertia.

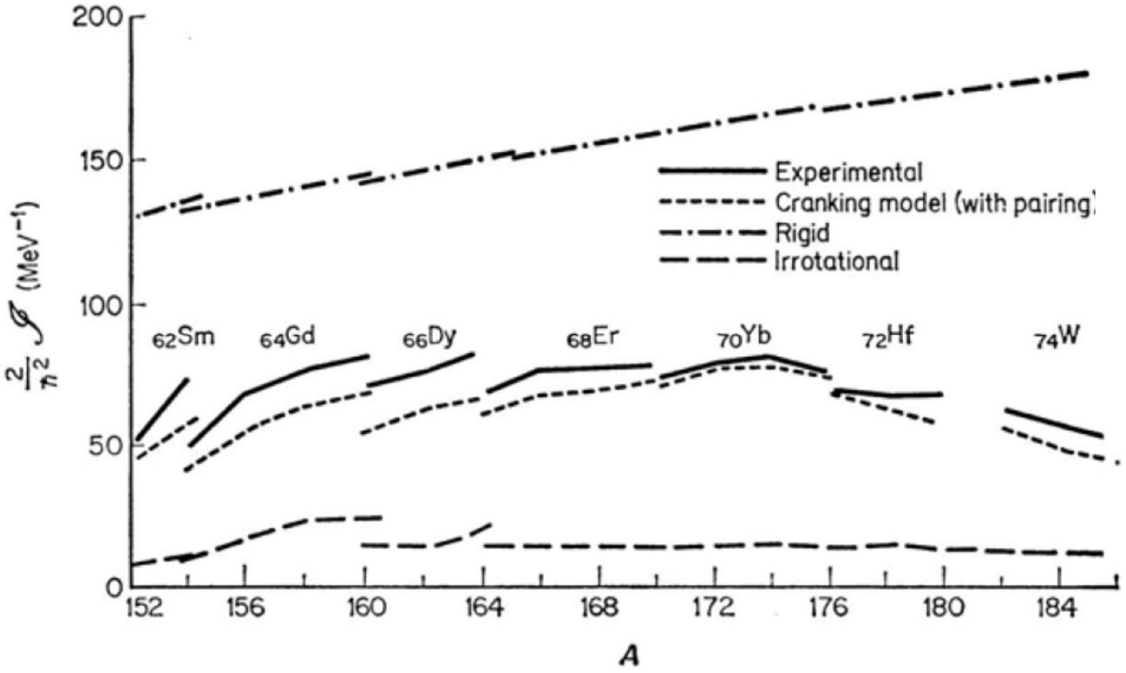

Irrotational, Rotational and Two Fluids picture

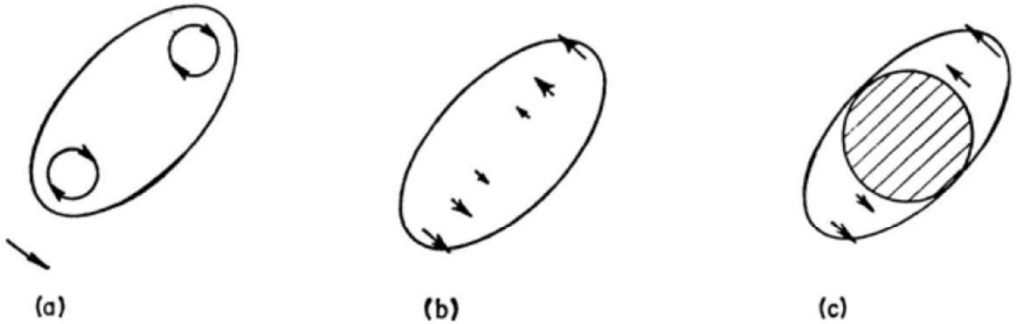

D.Rowe, Nucl. Coll. Motion, Dover.

$$\mathcal{J} = 2\hbar^2 \sum_{\mu\nu} \frac{|\langle\mu|J_x|\nu\rangle|^2 (U_\mu V_\nu - V_\mu U_\nu)^2}{E_\mu + E_\nu}$$

2. Nuclear Superfluidity: Moment of Inertia-2

Mottelson and Valatin [12] argued that there is a close formal correspondence between equations of motion in a constant magnetic field and in a rotating reference system. They suggested that critical magnetic field phenomena in superconductors should

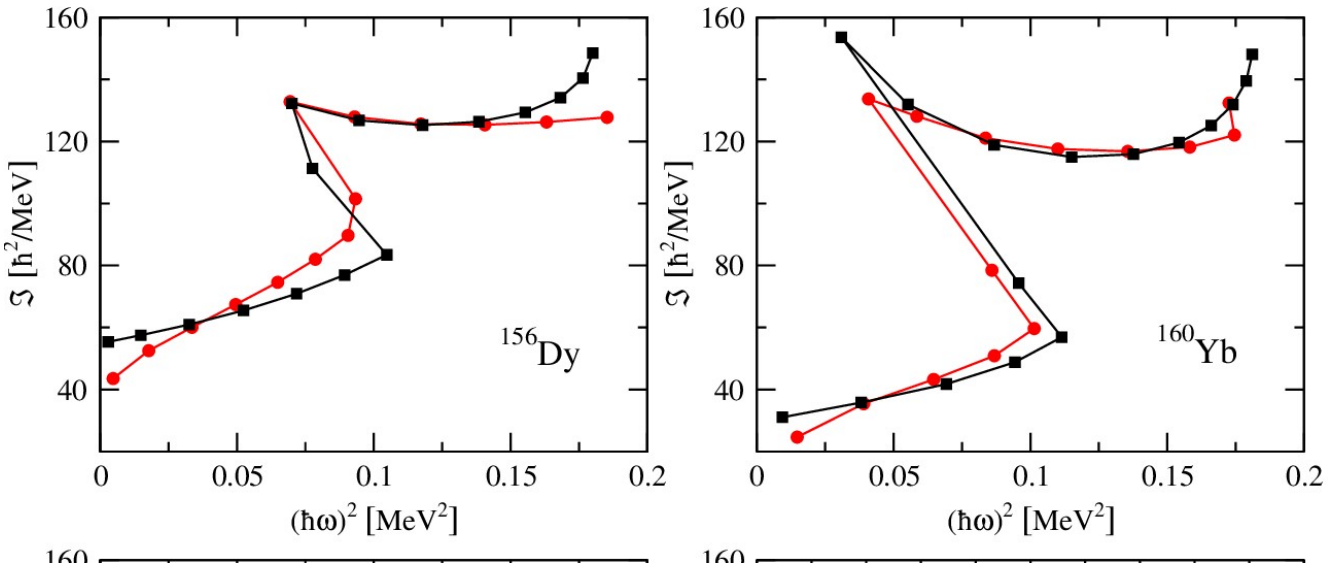

[12] B. R. Mottelson and J. G. Valatin, *Phys. Rev. Lett.* 5 (1960) 511.

A lesson: Nuclear superfluidity is not just Occupation Numbers.

It exhibits strong similarities with macroscopic superfluidity/superconductivity

2. Nuclear Superfluidity: the Gauge Angle

$$H' = H - \lambda n$$
$$= \sum_{\nu>0} (\varepsilon_\nu^{(0)} - \lambda)(a_\nu^\dagger a_\nu + a_{\bar{\nu}}^\dagger a_{\bar{\nu}}) - G \sum_{\mu,\nu>0} a_\mu^\dagger a_{\bar{\mu}}^\dagger a_{\bar{\nu}} a_\nu,$$

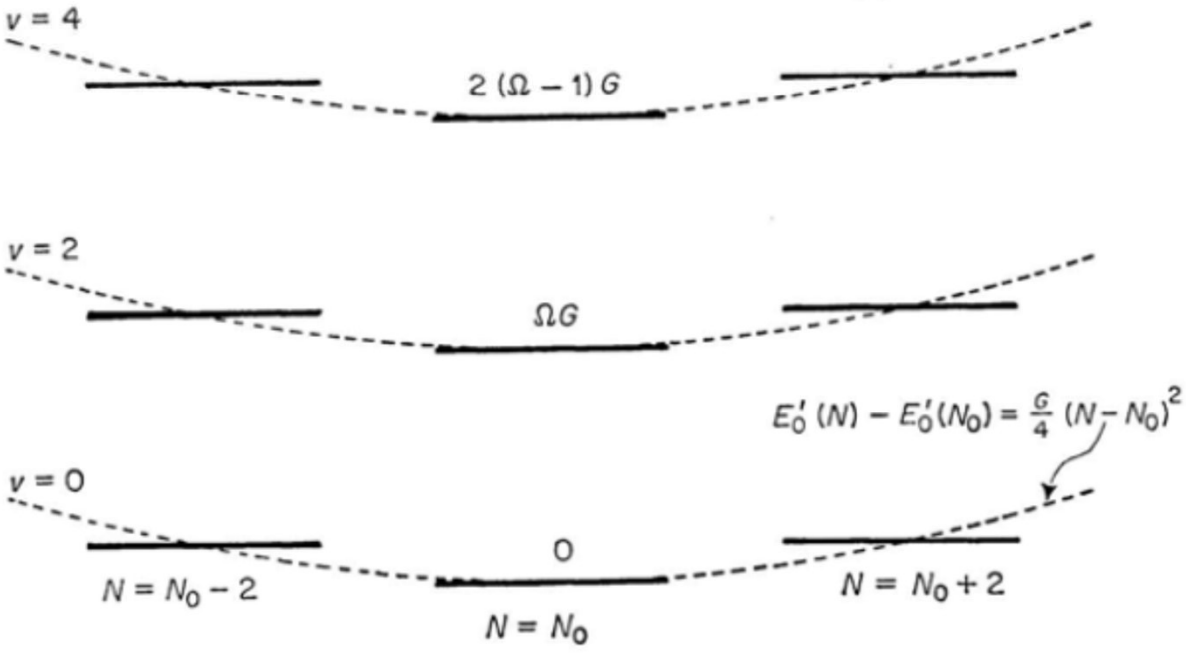

Figure 11.2. Exact energy spectrum for the Hamiltonian $H' = H - \lambda^{(N_0)} n$.

D.Rowe, Nucl. Coll. Motion, World Scientific

$$|BCS\rangle = \prod_k \left(U'_k + e^{-2i\phi} V'_k a^\dagger_{\mathbf{k}+\mathbf{s},\uparrow} a^\dagger_{-\mathbf{k}+\mathbf{s},\downarrow}\right)|0\rangle.$$

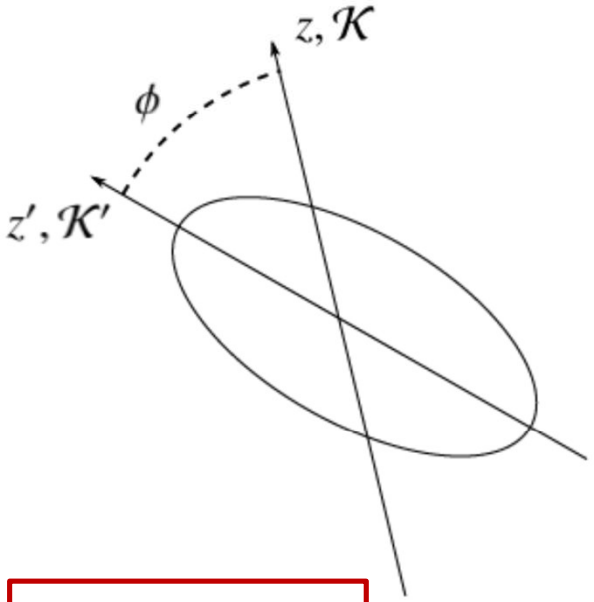

$$N = -i\frac{\partial}{\partial\phi}.$$

What is the phase coherence?

Incoherent (normal) crowd:
each electron for itself

Phase-coherent (superconducting) condensate
of electrons

2. Josephson Junctions (DC and AC): In Condensed Matter

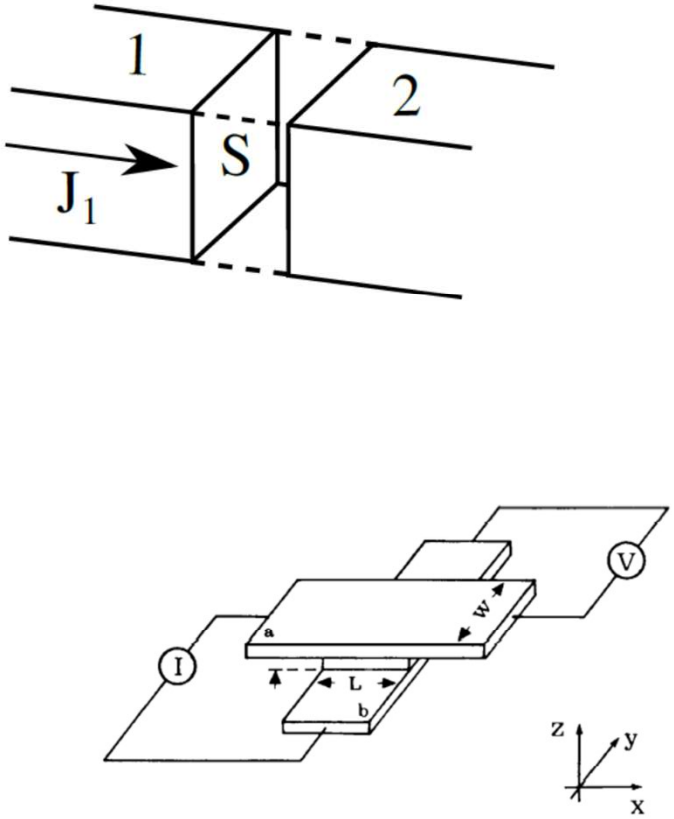

Figure 1.1 Tunneling junction of cross-type geometry. The dimensions are L and W; *a* and *b* are the two superconducting films.

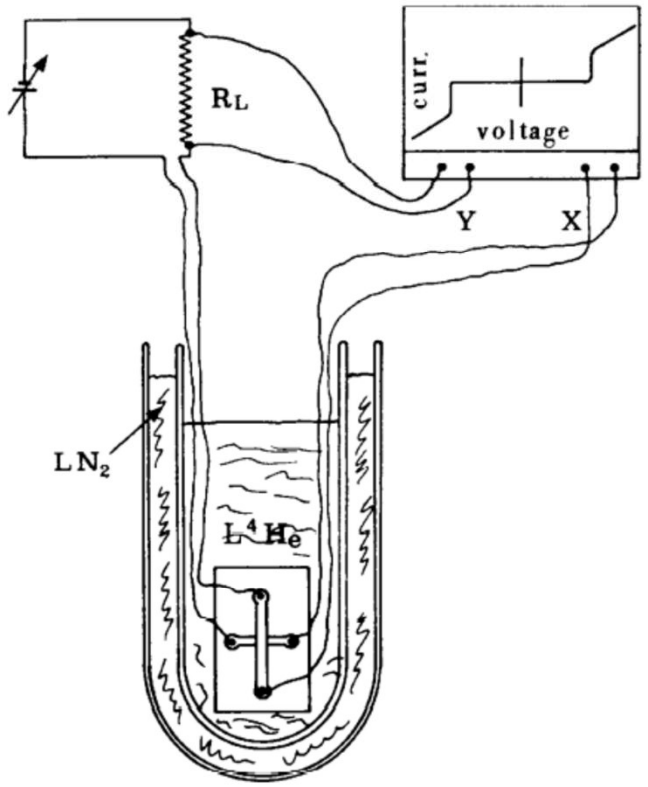

Figure 3.9 Schematic of the experimental apparatus used to measure the voltage-current characteristics of a junction. The inner dewar in which the sample is inserted is filled with liquid helium (L^4He), the outer dewar contains liquid nitrogen (LN_2).

3. Josephson Junctions (DC): A revision

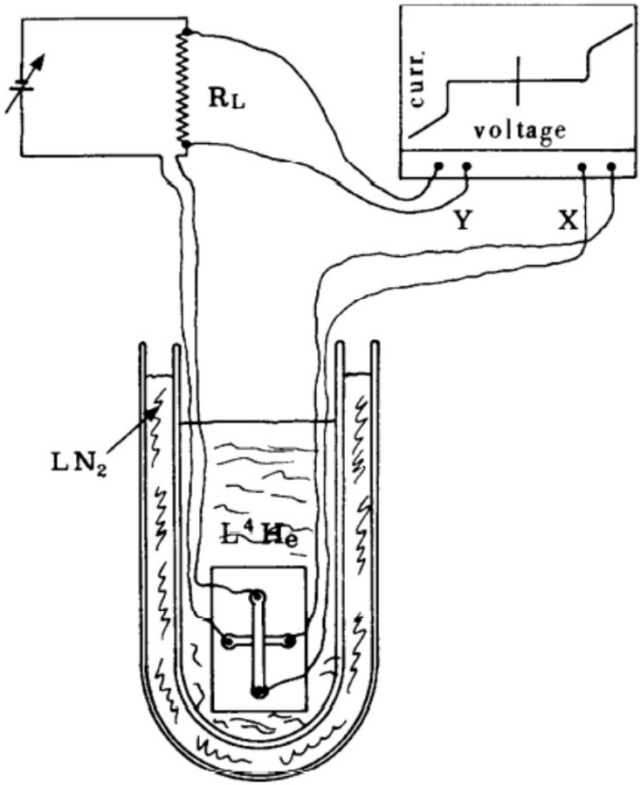

Figure 3.9 Schematic of the experimental apparatus used to measure the voltage-current characteristics of a junction. The inner dewar in which the sample is inserted is filled with liquid helium (L^4He), the outer dewar contains liquid nitrogen (LN_2).

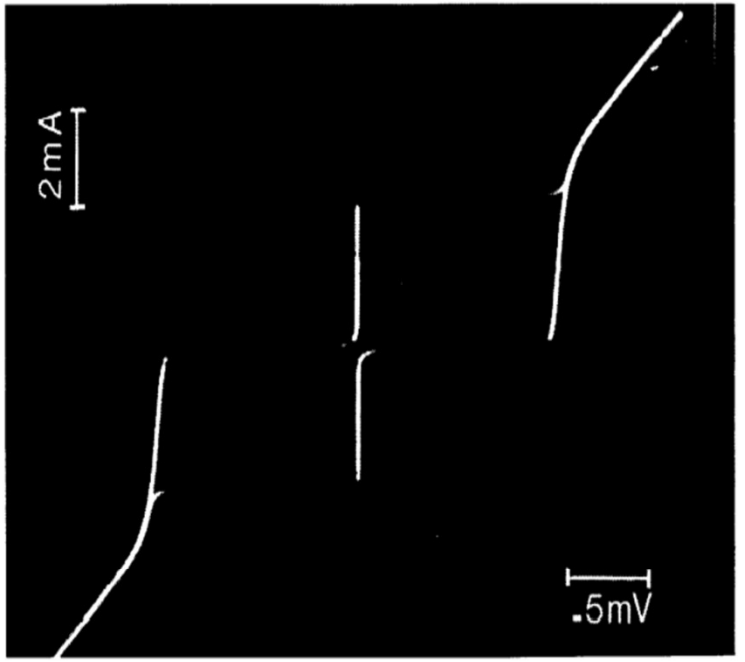

Figure 1.7 Typical voltage-current characteristic for a Sn-Sn_xO_y-Sn Josephson junction at $T=1.52$ K. Horizontal scale: 0.5 mV/div; vertical scale: 2 mA/div.

3. Josephson Junctions (DC and AC): In Condensed Matter

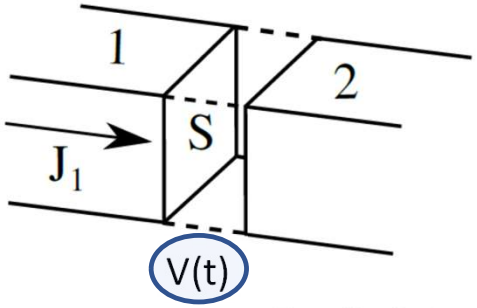

$$i\hbar\frac{\partial}{\partial t}\begin{pmatrix}\sqrt{n_A}e^{i\phi_A}\\ \sqrt{n_B}e^{i\phi_B}\end{pmatrix}=\begin{pmatrix}eV & K\\ K & -eV\end{pmatrix}\begin{pmatrix}\sqrt{n_A}e^{i\phi_A}\\ \sqrt{n_B}e^{i\phi_B}\end{pmatrix}$$

- **Tunneling between 2 weakly coupled superconductors strongly depends on the phase difference: $\theta = \theta_L - \theta_R$**

$$\dot{n}_A = \frac{2K\sqrt{n_A n_B}}{\hbar}\sin\varphi.$$

$$\frac{\partial\varphi}{\partial t}=\frac{2eV(t)}{\hbar}$$

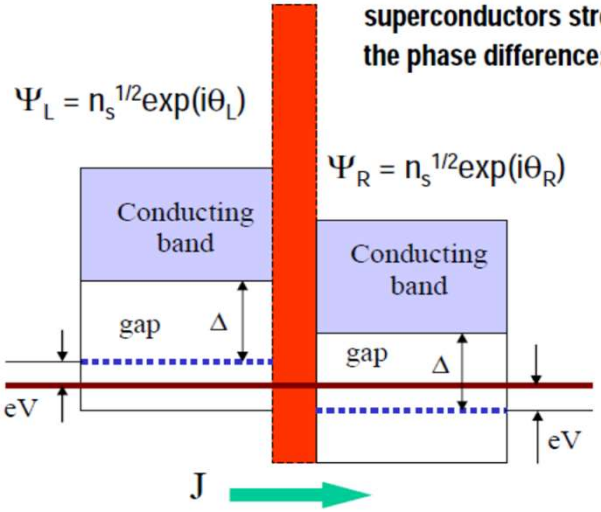

Because of the phase coherence, each superconductor behaves as a single-level quantum-mechanical system

$$I(t) = I_c\sin(\varphi(t))$$

$$\frac{\partial\varphi}{\partial t}=\frac{2eV(t)}{\hbar}$$

$$\varphi = \phi_B - \phi_A$$

3. Josephson Junctions (DC and AC): A revision.

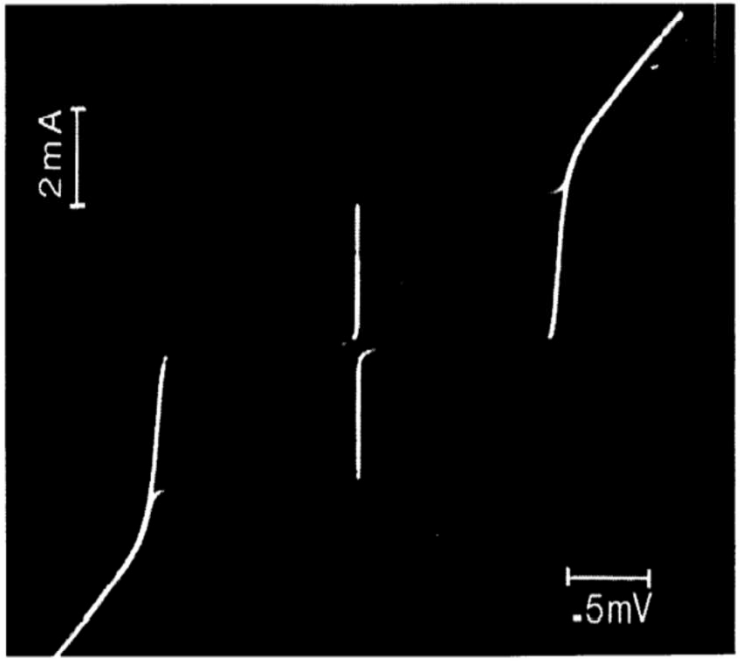

Figure 1.7 Typical voltage-current characteristic for a Sn-Sn_xO_y-Sn Josephson junction at $T = 1.52$ K. Horizontal scale: 0.5 mV/div; vertical scale: 2 mA/div.

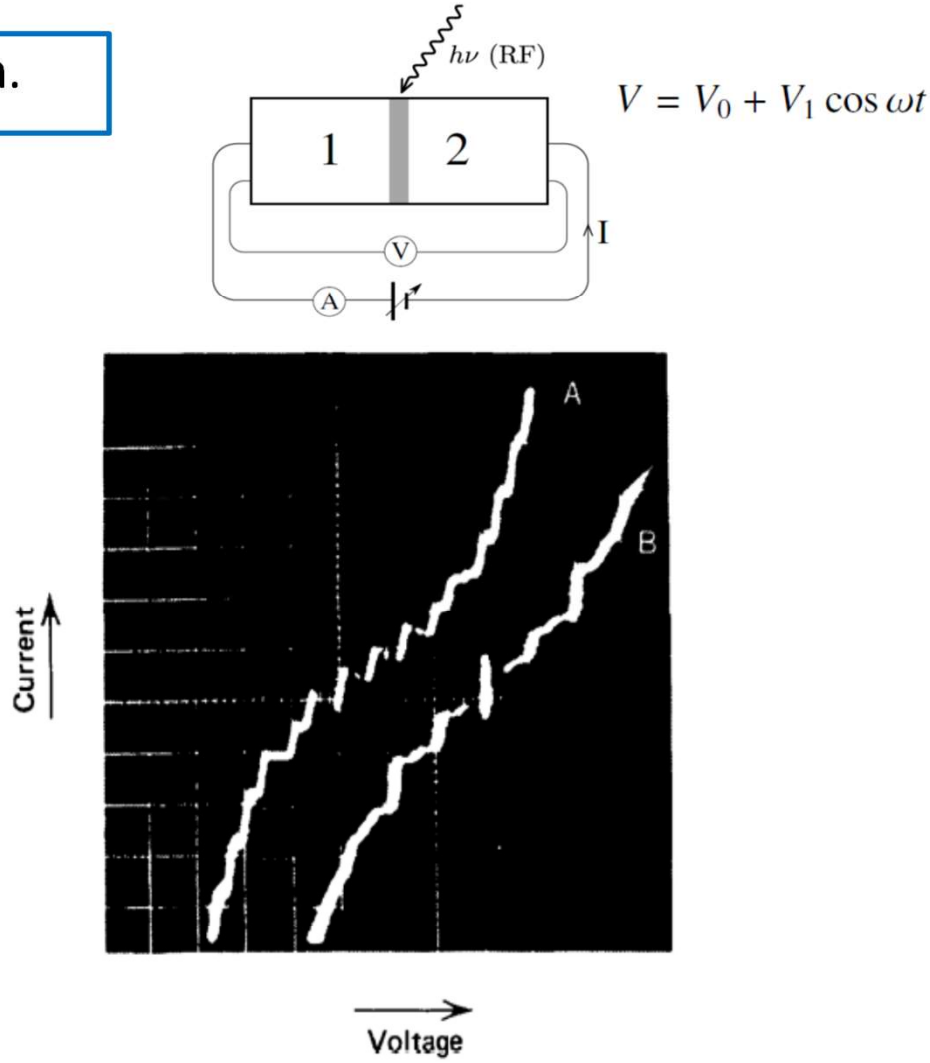

Figure 1.8 Microwave power at 9300 Mc/sec(A) and 24850 Mc/sec(B) produces many zero slope regions spaced at $h\nu/2e$ or $h\nu/e$. For A, $h\nu/e = 38.5$; for B, 103 μV. For A, horizontal scale is 58.8 μV/cm and vertical scale is 67 nA/cm; for B, horizontal scale is 50 μV/cm and vertical scale is 50 μA/cm. (After Shaprio 1963.)

3. Josephson Junctions (DC and AC): A revision.

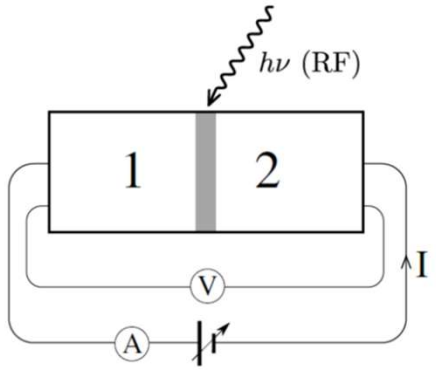

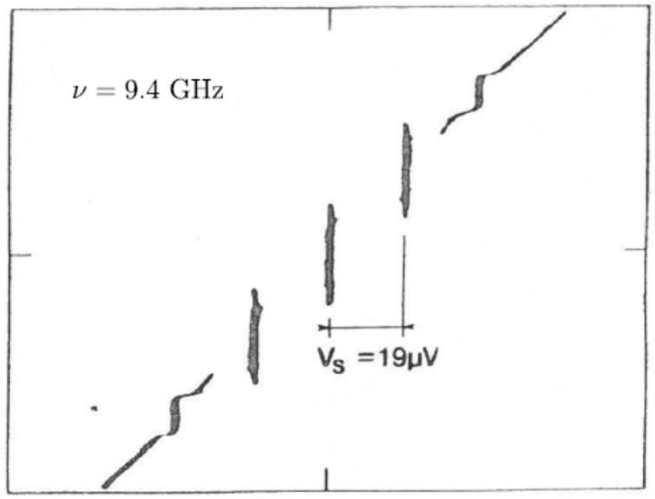

$$V = V_0 + V_1 \cos \omega t$$

$$\varphi(t) = \varphi_0 + n\omega t + a \sin(\omega t)$$

$$I(t) = I_c \sum_{m=-\infty}^{\infty} J_m(a) \sin(\varphi_0 + (n+m)\omega t)$$

Oscilloscope presentation of current-versus-voltage characteristics of a tunnel junction at 4.2 K formed by an Al tip on a $(La_{0.925}Sr_{0.075})_2CuO_4$ sample ([82]). Steps induced by incident microwave radiation at 9.4 GHz, implying $V_0 = V_S = kK_J\nu = k \times 2.07 \times 10^{-12}$ mV s$\times 9.4 \times 10^9$ s^{-1} = 19.4 μV$\times k$ ($k = 0, \pm 1, \pm 2, \ldots$).

3. Josephson Junctions (DC and AC): A revision.

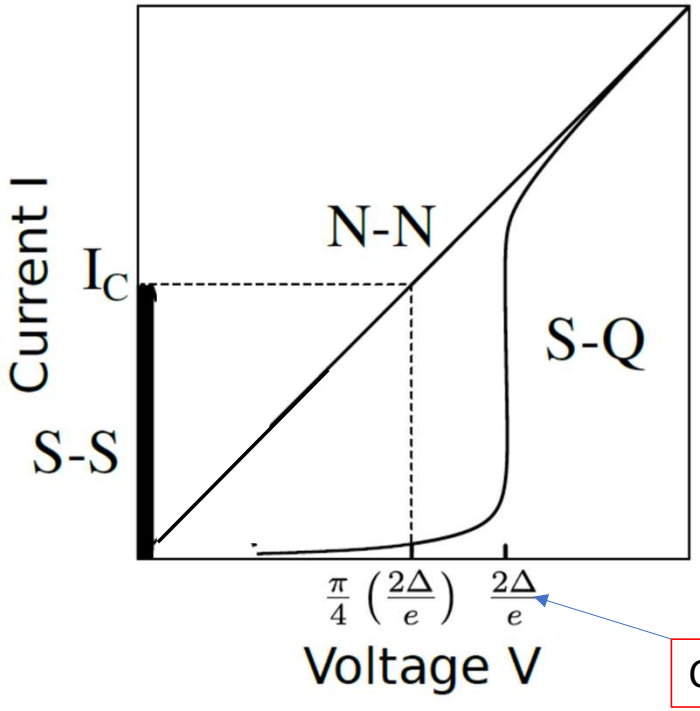

Critical bias voltage

$$J = J_c \sin\left(\phi_{rel}(0) - \left(\frac{2eV}{\hbar} t\right)\right)$$

$$\omega_J = \frac{2eV}{\hbar}.$$

4. The Legnaro's 116Sn+60Ni 2NT and 1NT data at different E_cm:

PRL 113, 052501 (2014) PHYSICAL REVIEW LETTERS week ending 1 AUGUST 2014

Neutron Pair Transfer in ^{60}Ni + ^{116}Sn Far below the Coulomb Barrier

D. Montanari,[1] L. Corradi,[2] S. Szilner,[3] G. Pollarolo,[4] E. Fioretto,[2] G. Montagnoli,[1] F. Scarlassara,[1] A. M. Stefanini,[2] S. Courtin,[5] A. Goasduff,[5,6] F. Haas,[5] D. Jelavić Malenica,[3] C. Michelagnoli,[2] T. Mijatović,[3] N. Soić,[3] C. A. Ur,[1] and M. Varga Pajtler[7]

FIG. 3 (color online). Top: Ratio between the quasielastic and the Rutherford cross section. Symbols represent the experimental values, solid line is the theoretical calculation with the GRAZING code. Bottom: Experimental (points) and microscopically calculated (lines) transfer probabilities for the one- (^{61}Ni) and two-neutron (^{62}Ni) pickup plotted as a function of the distance of closest approach D (the entrance channel Coulomb barrier is estimated to be at 12.13 fm [4]). We also report (top) the reduced distance $d_0 = D/(A_1^{1/3} + A_2^{1/3})$. The shown errors are only statistical and in most cases are smaller than the size of the symbol.

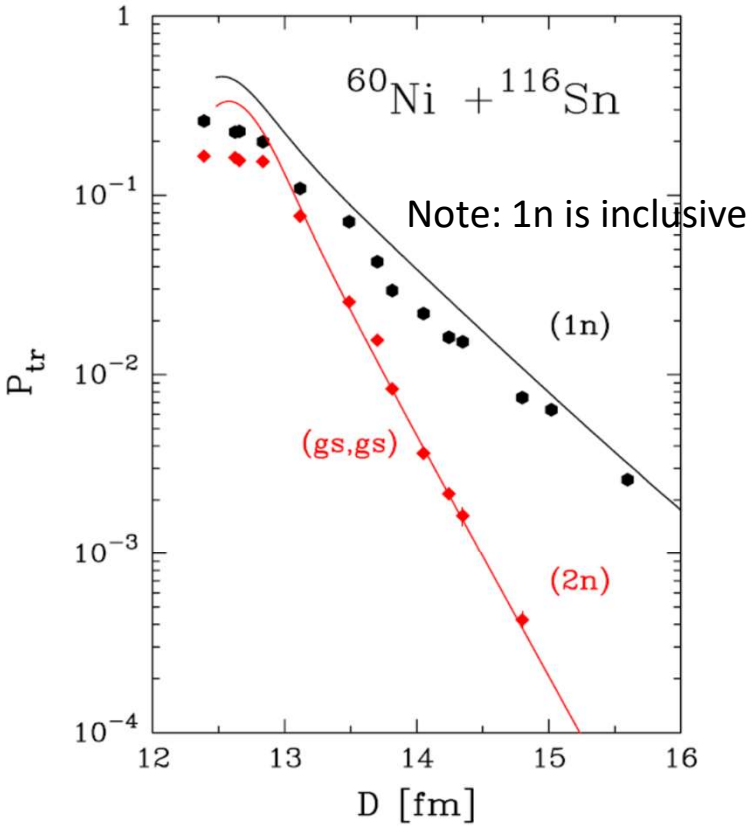

Note: 1n is inclusive

Semiclassical calculations in this paper

4. The Legnaro's 116Sn+60Ni 2NT and 1NT data at different E_cm:

PRL 113, 052501 (2014) PHYSICAL REVIEW LETTERS week ending 1 AUGUST 2014

Neutron Pair Transfer in ^{60}Ni + ^{116}Sn Far below the Coulomb Barrier

D. Montanari,[1] L. Corradi,[2] S. Szilner,[3] G. Pollarolo,[4] E. Fioretto,[2] G. Montagnoli,[1] F. Scarlassara,[1] A. M. Stefanini,[2] S. Courtin,[5] A. Goasduff,[5,6] F. Haas,[5] D. Jelavić Malenica,[3] C. Michelagnoli,[2] T. Mijatović,[3] N. Soić,[3] C. A. Ur,[1] and M. Varga Pajtler[7]

D_0(fm)	E_{cm} (MeV)	$(E_B - E_{cm})$ (MeV)	$\left(\frac{4}{\pi}\right)^2 \left(\frac{\sigma_{2n}}{\sigma_{1n}}\right)$
13.12	158.63	-1.03	1.14
13.49	154.26	3.34	0.57
13.70	151.86	5.74	0.59
13.81	150.62	6.98	0.46
14.05	148.10	9.50	0.27
14.24	146.10	11.50	0.22
14.39	145.02	12.58	0.18

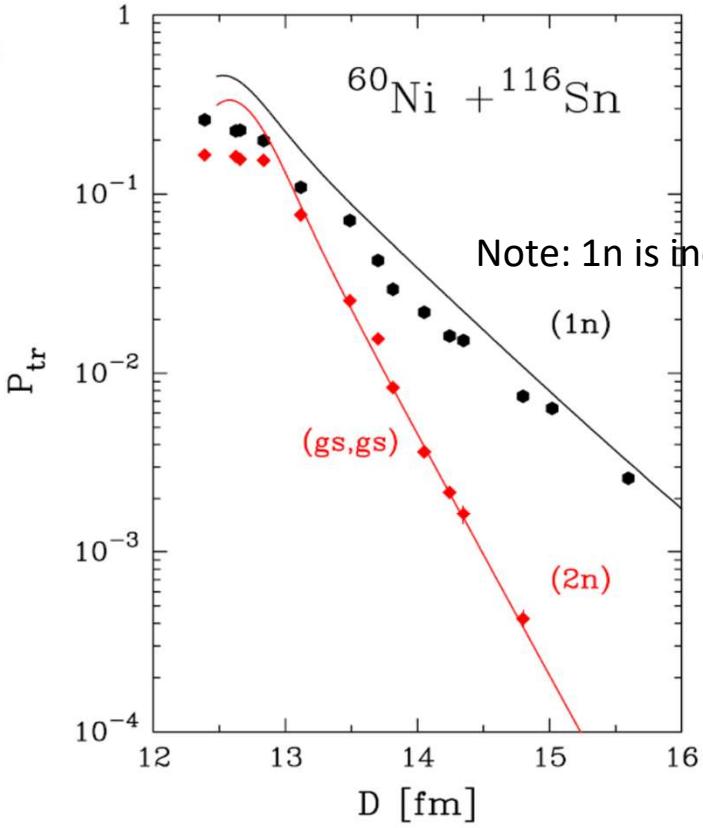

Note: 1n is inclusive

4. The Legnaro's 116Sn+60Ni 2NT and 1NT data at different E_cm:

4.1 DWBA analysis.

$$T(\mathbf{k}_f,\mathbf{k}_i) = 2\sum_{KM}\sum_{j_i,j_f} B^{(A)*}_{j_f} B^{(b)}_{j_i} \int \chi^*_f(\mathbf{r}_{Bb},\mathbf{k}_f)\left[\phi^{(A)}_{j_f}(\mathbf{r}_{A_2})\phi^{(A)}_{j_f}(\mathbf{r}_{A_1})\right]^{0*}_{0} U^{(A)}(r_{b1})\left[\phi^{(A)}_{j_f}(\mathbf{r}_{A_2})\phi^{(b)}_{j_i}(\mathbf{r}_{b_1})\right]^{K}_{M} d\mathbf{r}_{Cc}\, d\mathbf{r}_{b_1}\, d\mathbf{r}_{A_2}$$

$$\times \int G(\mathbf{r}_{Cc},\mathbf{r}'_{Cc})\left[\phi^{(A)}_{j_f}(\mathbf{r}'_{A_2})\phi^{(b)}_{j_i}(\mathbf{r}'_{b_1})\right]^{K*}_{M} U^{(A)}(r'_{b2})\left[\phi^{(b)}_{j_i}(\mathbf{r}'_{b_2})\phi^{(b)}_{j_i}(\mathbf{r}'_{b_1})\right]^{0}_{0} \chi_i(\mathbf{r}'_{Aa},\mathbf{k}_i)\, d\mathbf{r}'_{Cc}\, d\mathbf{r}'_{b_1}\, d\mathbf{r}'_{A_2},$$

$$B_j = \sqrt{\frac{(2j+1)}{2}}\, U'_j V'_j,$$

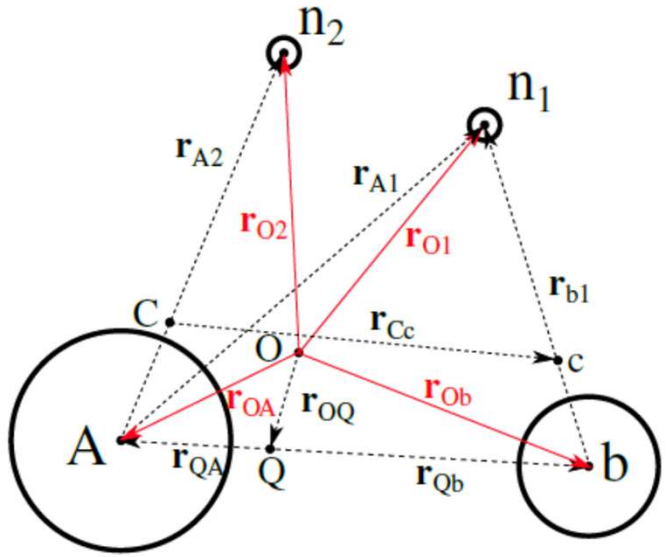

4. The Legnaro's 116Sn+60Ni 2NT and 1NT data at different E_cm: DWBA results

$$^{116}\mathrm{Sn} + ^{60}\mathrm{Ni} \rightarrow \begin{cases} ^{115}\mathrm{Sn} + ^{61}\mathrm{Ni} & (Q_{1n} = -1.74\ \mathrm{MeV}) \\ ^{114}\mathrm{Sn} + ^{62}\mathrm{Ni} & (Q_{2n} = 1.307\ \mathrm{MeV}), \end{cases}$$

MAIN INGREDIENTS

Montanari's Opt. Potentials (Pollarollo)

G=25/A MeV

s-p levels from WS potentials

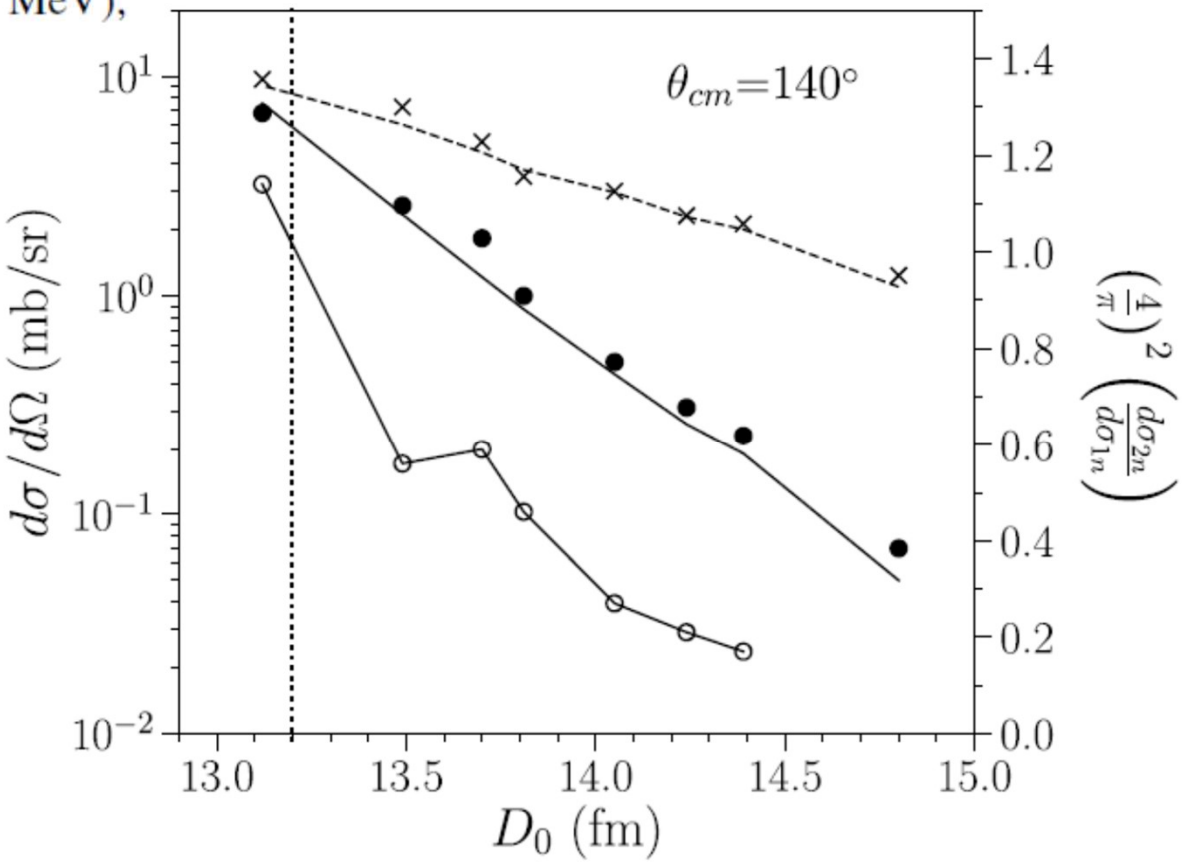

5. Gamma emission in 2NT channel

$$T_{m_\gamma}(\mathbf{k}_f,\mathbf{k}_i)=\sum_{j_i,j_f} B_{j_i}B_{j_f}\int \chi^{*}_{f}(\mathbf{r}_{Bb};\mathbf{k}_f)\left[\phi_{j_f}(\mathbf{r}_{A_1})\phi_{j_f}(\mathbf{r}_{A_2})\right]^{0*}_{0} D_{m_\gamma}\left[\phi_{j_f}(\mathbf{r}_{A_2})\phi_{j_f}(\mathbf{r}_{b_1})\right]^{K}_{M} v(r_{b1})d\mathbf{r}_{Cc}\,d\mathbf{r}_{b_1}\,d\mathbf{r}_{A_2}$$

$$\times\int G(\mathbf{r}_{Cc},\mathbf{r}'_{Cc})\left[\phi_{j_f}(\mathbf{r}'_{A_2})\phi_{j_i}(\mathbf{r}'_{b_1})\right]^{K*}_{M} v(r'_{c2})\left[\phi_{j_i}(\mathbf{r}'_{b_2})\phi_{j_i}(\mathbf{r}'_{b_1})\right]^{0}_{0}\chi_i(\mathbf{r}'_{Aa};\mathbf{k}_i)\,d\mathbf{r}'_{cC}\,d\mathbf{r}'_{b_1}\,d\mathbf{r}'_{A_2}.$$

$$\mathbf{D}_{m_\gamma}=e_{eff}\sqrt{\frac{4\pi}{3}}\left(r_{O1}Y^1_{m\gamma}(\hat{r}_{O1})+r'_{O2}Y^1_{m\gamma}(\hat{r}'_{O2})\right) \quad ;\ e_{eff}=-e\frac{(Z_A+Z_b)}{A_A+A_b}$$

$$\mathcal{T}^q(\mathbf{k}_\gamma,\mathbf{k}_f)=\sum_{m_\gamma}\mathcal{D}^1_{m_\gamma q}(R_\gamma)\,T_{m_\gamma}(\mathbf{k}_f,\mathbf{k}_i).$$

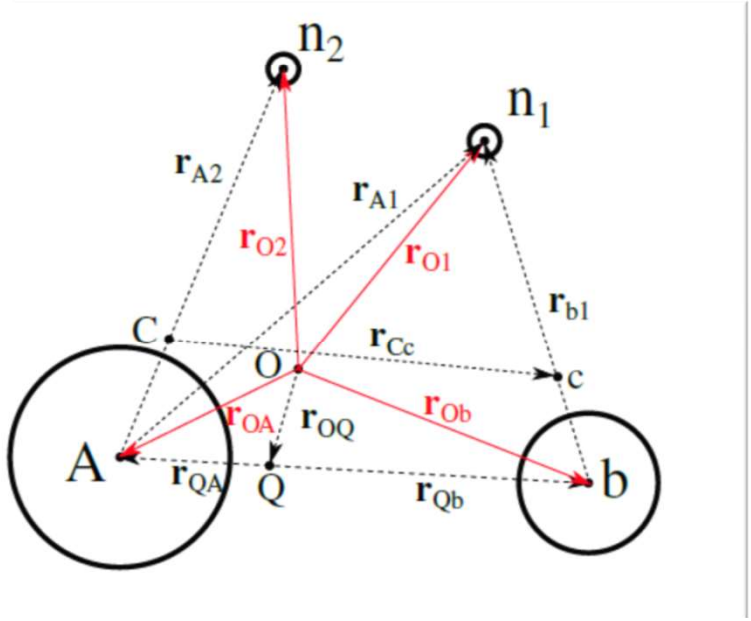

$$\frac{d^3\sigma^{\gamma}_{2n}}{d\Omega_\gamma d\Omega dE_\gamma}=\rho_f(E_f)\rho_\gamma(E_\gamma)\left(\left|\mathcal{T}^1(\mathbf{k}_\gamma,\mathbf{k}_f)\right|^2+\left|\mathcal{T}^{-1}(\mathbf{k}_\gamma,\mathbf{k}_f)\right|^2\right)\delta(E_i-E_\gamma-E_f+Q)$$

$$=\frac{\mu_i\mu_f}{(2\pi\hbar^2)^2}\frac{k_f}{k_i}\left(\frac{E^2_\gamma}{(\hbar c)^3}\right)\left(\left|\mathcal{T}^1(\mathbf{k}_\gamma,\mathbf{k}_f)\right|^2+\left|\mathcal{T}^{-1}(\mathbf{k}_\gamma,\mathbf{k}_f)\right|^2\right)\delta(E_i-E_\gamma-E_f+Q).$$

5. Gamma emission in Legnaro's 116Sn+60Ni 2NT channel

PHYSICAL REVIEW C **103**, L021601 (2021)

Letter | Editors' Suggestion | Featured in Physics

Quantum entanglement in nuclear Cooper-pair tunneling with γ rays

G. Potel,[1] F. Barranco,[2] E. Vigezzi,[3] and R. A. Broglia[4,5]

$$V_J^N = Q_{2n}/2e_{eff}$$

$$\omega_J = \frac{2eV^N}{\hbar}.$$

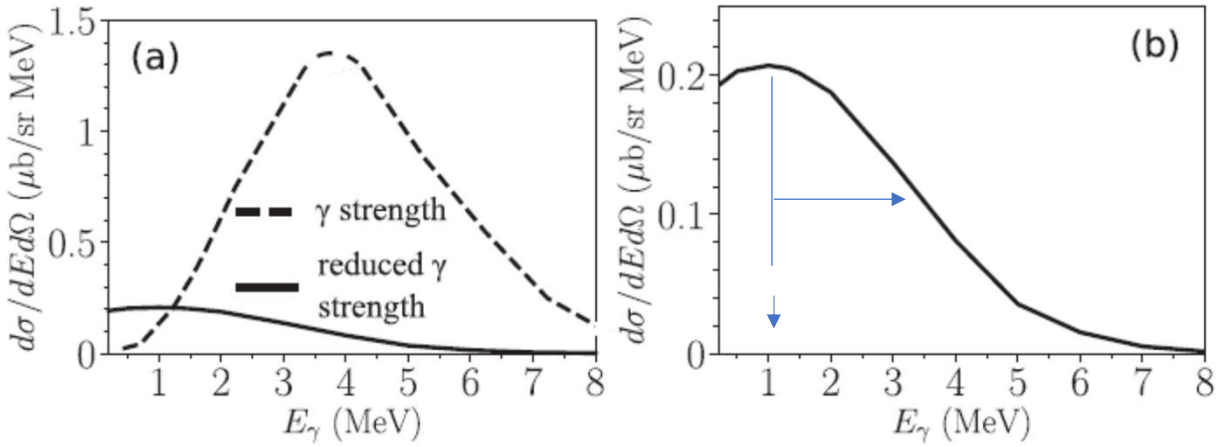

The reduced strength shows a maximum at about 1.2MeV (Q2n=1.3MeV!!) , and a width Γ/2 = 2 MeV

5. Gamma emission in Legnaro's 116Sn+60Ni 2NT channel: Gamma emmission angular distribution

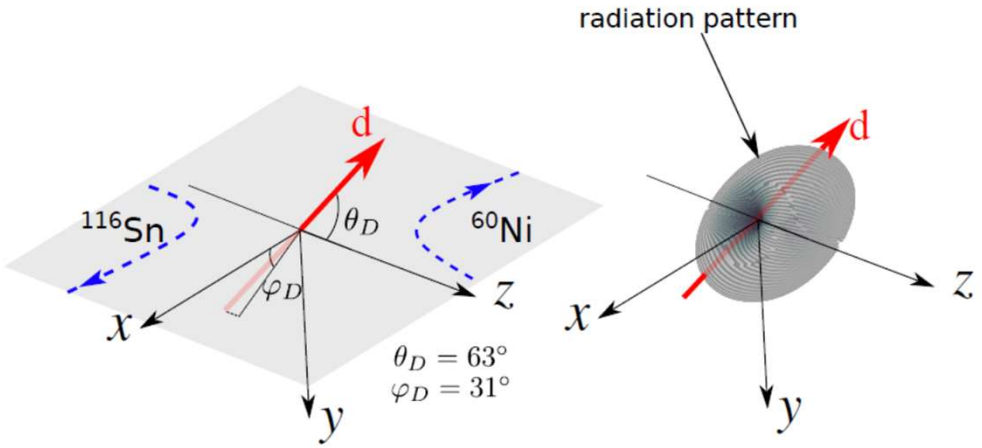

- The angular radiation pattern reflects the orientation of the dipole, providing novel insight into the reaction mechanism.
- The polarization of the emitted photons can also provide valuable information.

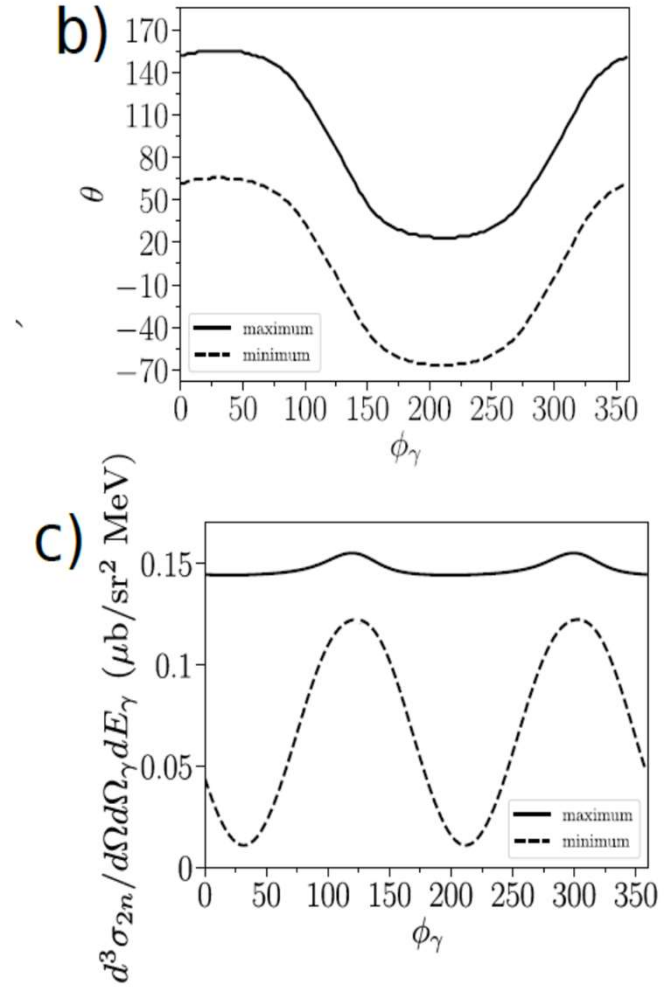

5. Gamma emission in Legnaro's 116Sn+60Ni 2NT **versus 1NT channel**

2n-transfer

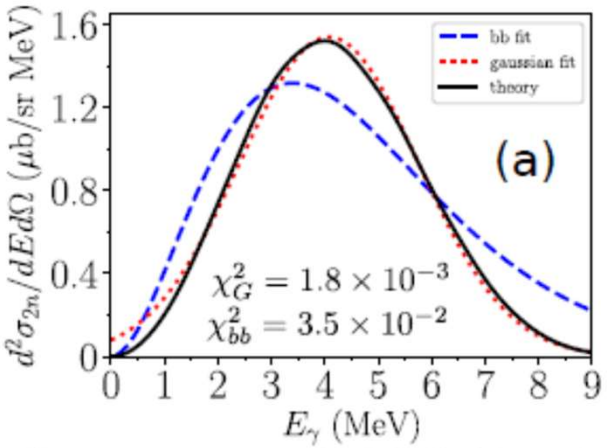

Gaussian: $\sigma = 1.67$ MeV, $E_0 = 4.08$ MeV

1n-transfer

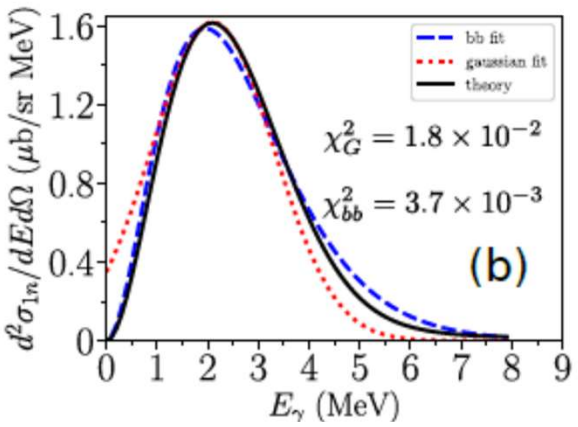

black body: $T = 0.69$ MeV

PHYSICAL REVIEW C **105**, L061602 (2022)

Letter | Editors' Suggestion

Transient Joule- and (ac) Josephson-like photon emission in one- and two- nucleon tunneling processes between superfluid nuclei: Blackbody and coherent spectral functions

5. Gamma emission in the 2NT channel: The future experiment at Legnaro.

PIAVE-ALPI ACCELERATOR

Search for a Josephson-like effect in the ^{116}Sn+^{60}Ni system
PRISMA + AGATA experiment

Spokesperson(s): L. Corradi, S. Szilner

L. Corradi[1], E. Fioretto[1], F. Galtarossa[1], A. Goasduff[1], A. Gottardo[1], A. M. Stefanini[1], J. J. Valiente-Dobón[1], G. Montagnoli[2], D. Mengoni[2], M. del Fabbro[2], F. Scarlassara[2], S. Szilner[3], J. Diklić[3], D. Jelavić Malenica[3], T. Mijatović[3], M. Milin[4], G. Benzoni[5], S. Bottoni[6,5], A. Bracco[6,5], F. Camera[6,5], F. Crespi[6,5], R. Depalo[6,5], E. Gamba[6,5], S. Leoni[6,5], B. Million[5], O. Wieland[5], M. Caamano[7], Y. Ayyad[7], F. Barranco[8], G. Pollarolo[9], G. Potel[10], E. Vigezzi[5], R. A. Broglia[11,6]

. The purpose of the proposed experiment is to probe and measure such γ-rays. The measurement will be performed in inverse kinematics at E_{lab} = 452.5 MeV by detecting Ni-like recoils with PRISMA at $\theta_{lab} = 20°$ in coincidence with γ rays detected with AGATA and with an additional array of $LaBr_3$:(Ce) scintillators. The presence of the predicted γ-rays would provide evidence that specific effects in superconductivity [B.D. Josephson, Phys. Lett. 1, 251 (1962)], directly probed so far for macroscopic objects, may also be found at the femtometer scale.

We ask for a total of **15 days** of beam time with **PIAVE+ALPI**.

6. Role of the the barrier thickness d and bias potential V in Josephson Junctions: A revision.

Controlling the thickness of Josephson tunnel barriers with atomic layer deposition

Alan J. Elliot, Chunrui Ma, Rongtao Lu, Melisa Xin, Siyuan Han, Judy Z. Wu, Ridwan Sakidja, Haifeng Yu

arXiv:1408.3077v1

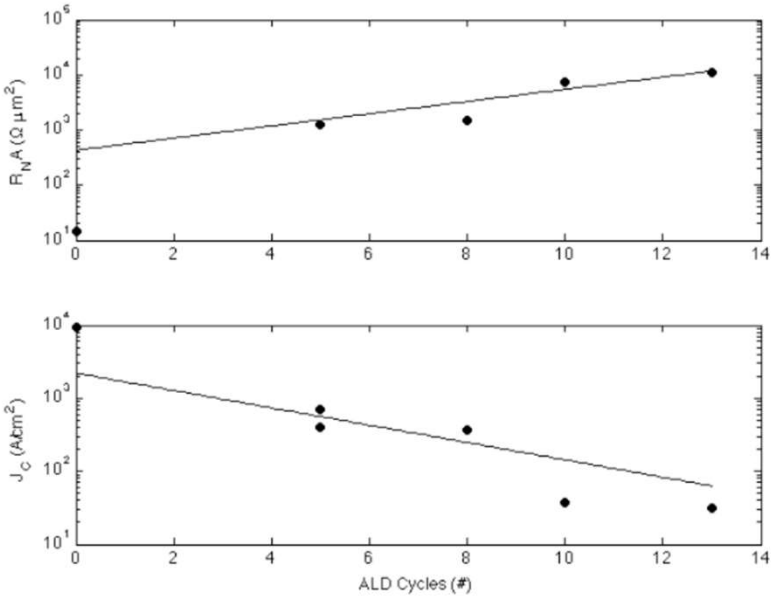

Fig. 3: Specific tunnel resistance vs ALD cycles (a), and projected J_C vs ALD cycles (B). The data point at 0 is from Reference [16] and was not included in the fits.

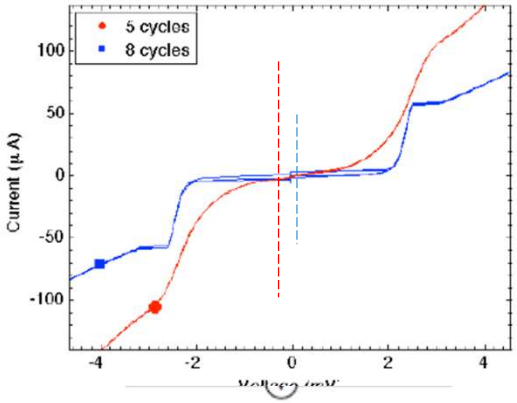

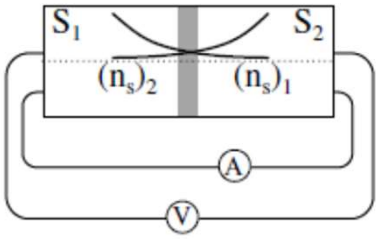

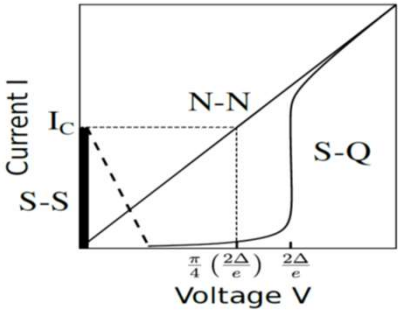

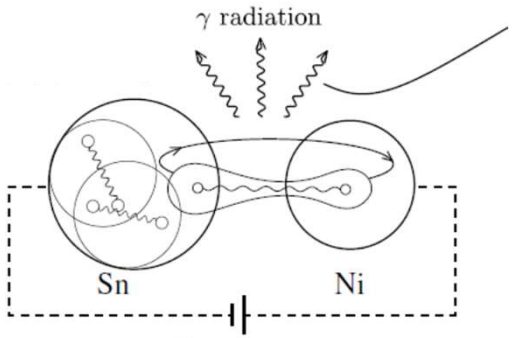

$V^N = Q_{2n}/2e_{eff}$

nuclear superconducting "circuit"

6. Velocity of the Transferred Cooper and (critical) Depairing velocity .

BUT….!

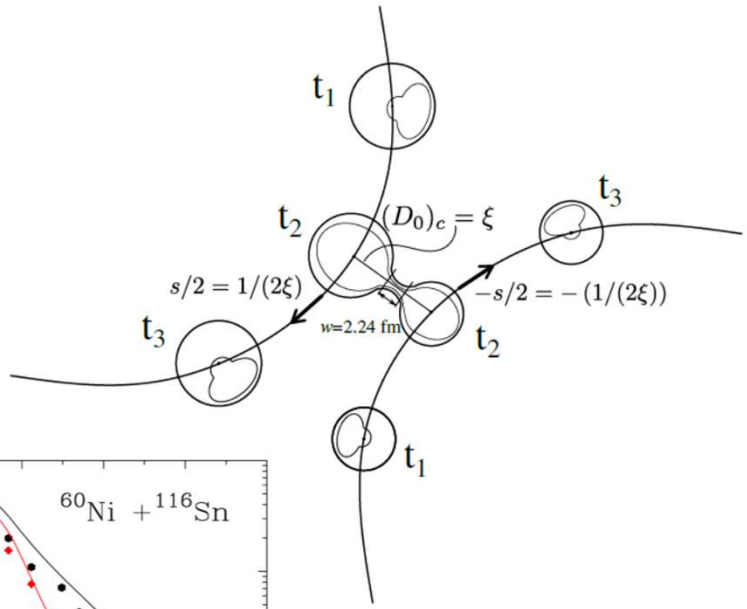

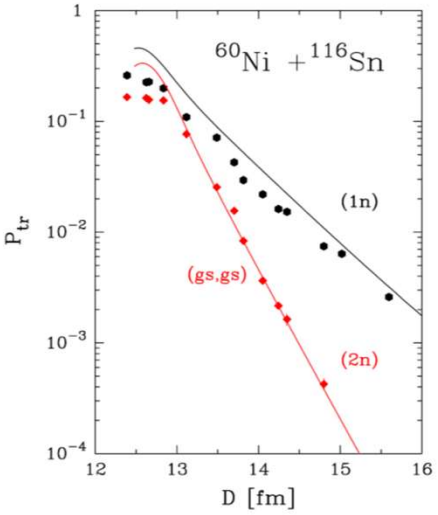

$$v_c = \frac{2\Delta}{mv_F} = \frac{\hbar}{m\xi}$$

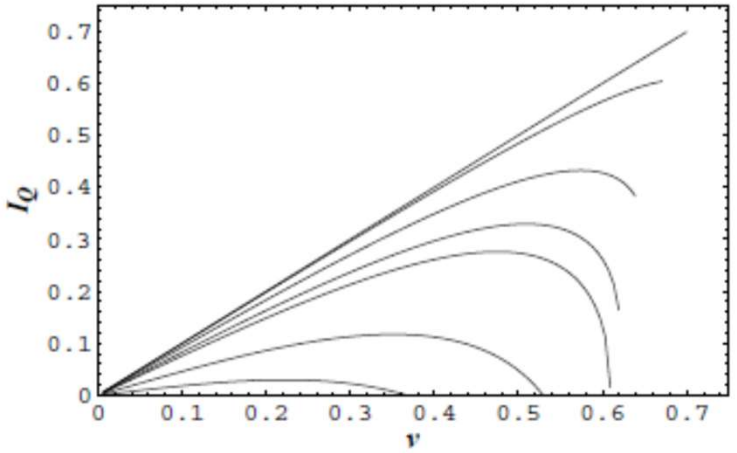

FIG. 5: Supercurrent I_Q (in units of I_Q^0) vs. superfluid velocity v (in unit of v_L) for various temperatures. From top to bottom: $T = (0.1, 0.25, 0.4, 0.5, 0.556, 0.75, 0.9)\, T_c^0$. The curves terminate at the critical velocities $v_c(T)$ appropriate to these temperatures. The maximum supercurrent for a particular curve determines the value of the critical current at that temperature.

Revisiting the critical velocity of a clean one-dimensional superconductor

Tzu-Chieh Wei

*Institute for Quantum Computing and Department of Physics and Astronomy, University of Waterloo, Waterloo, ON N2L 3G1, Canada**

Paul M. Goldbart

Department of Physics, Institute for Condensed Matter Theory, and Federick Seitz Materials Research Laboratory, University of Illinois at Urbana-Champaign, Urbana, Illinois 61801, U.S.A.

(Dated: April 15, 2009)

6. Velocity of the Transfered (nuclear) Cooper Pair larger than the critical depairing velocities leads to P2 < P1

If the Cooper-pair velocity between the nuclei is larger than v_crit

Cooper pairs breaking is most likely → P1 > P2 …… (Do > Do_crit)

Conversely if P2 > P1 Cooper pairs velocity is smaller than v_cri....(Do < Do_crit)

When P2 = P1 one can see that in fact both velocities are equal (Critical situation)

Cooper pair velocity

thickness of the barrier

Collision time

$$\frac{(D_0)_c - (R(^A) + R(^b) + a)}{\tau_{coll}} = \frac{2\Delta}{m v_F}$$

Broglia et al. arXiv:2206.05351

Critical Depairing velocity

SUMMARY

116Sn + 60Ni 2NT reaction at Ecm=154.3MeV may be considered a (critical) J-Junction

Gamma emission of S-S and of S-Q type are predicted

Depairing velocity appears as a leading mechanism at Do > Do_crit. (Ecm<154.3MeV)

SUPER SUMMARY

Physics VIEWPOINT

The Tiniest Superfluid Circuit in Nature

A new analysis of heavy-ion collision experiments uncovers evidence that two colliding nuclei behave like a Josephson junction—a device in which Cooper pairs tunnel through a barrier between two superfluids.

By Piotr Magierski

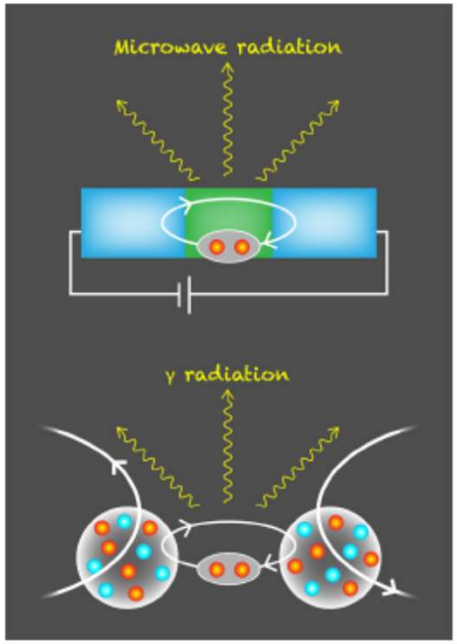

THANK YOU !!

FB acknowledges PID2020-114687GB-I00, funded by MCIN/AEI/10.13039/501100011033

GP acknowledges U.S. Department of Energy by Lawrence Livermore National Laboratory under Contract No. DEAC52-07NA27344.

Consider two even nuclei A and B in their ground states in close proximity with fixed positions. The internal state of the system is denoted by $|0\rangle$. The ground states of

$$\Psi = \sum_N a_N |N\rangle. \qquad H_t|N\rangle = -\frac{1}{2}J_0(|N+1\rangle + |N-1\rangle)$$

$$\Psi = \sum_N e^{iN\phi}|N\rangle, \qquad E = -J_0 \cos\phi.$$

$$f(\phi) = \frac{1}{\sqrt{2\pi}}\sum a_N e^{iN\phi}, \quad \text{where} \quad a_N = \frac{1}{\sqrt{2\pi}}\int_0^{2\pi} e^{-iN\phi} f(\phi) \qquad N = -i\frac{\partial}{\partial\phi}.$$

A more general hamiltonian has a term depending on the number of pairs moved as well as the transfer term (5.2)

$$H = H_t + \epsilon(N). \tag{5.6}$$

The term $\epsilon(N)$ is the total ground state energy of the two nuclei when N pairs have been transferred. The Schrödinger equation with the hamiltonian (5.6) can not be solved analytically for a general ϵN but the Heisenberg equations of motion for the operators ϕ and N have an interesting form. They are

$$\mathrm{i}\hbar\frac{\mathrm{d}N}{\mathrm{d}t} = [N, H] = [N, H_t] = \mathrm{i}J_0\frac{\mathrm{d}\cos\phi}{\mathrm{d}\phi}$$

$$\mathrm{i}\hbar\frac{\mathrm{d}\phi}{\mathrm{d}t} = [\phi, H] = [\phi, \epsilon(N)] = \mathrm{i}\frac{\mathrm{d}\epsilon(N)}{N}$$

and simplify to give

$$\frac{\mathrm{d}N}{\mathrm{d}t} = -(J_0/\hbar)\sin\phi, \qquad \frac{\mathrm{d}\phi}{\mathrm{d}t} = \epsilon'(N)/\hbar. \tag{5.7}$$

These are Josephson's two relations. The first connects the Josephson tunnelling current with the gauge angle and the second gives the rate of change of ϕ in terms of the potential difference between A and B.

DC “Nuclear supercurrent”

The transfer ampiltude J_0 is time dependent for pair transfer between heavy ions. It is small when the nuclei are far appart and a maximum at the point of closest approach. We can write a time dependent Schrödinger equation for the wave function $f(\phi)$ in the gauge representation as

$$i\hbar\frac{\partial f}{\partial t} = H_t f = -J_0(t)\cos(\phi) f, \tag{5.8}$$

where we have used the form of H_t in the gauge repesentation give in equation (5.3). It should be solved with the initial condition $N = 0$, ($f(\phi) = 1/\sqrt{2\pi}$ as $t \to -\infty$. The solution as $t \to +\infty$ is

$$f(\phi) = \frac{1}{\sqrt{2\pi}} e^{ix\cos\phi}, \quad \text{with} \quad x = \frac{1}{\hbar}\int_{-\infty}^{\infty} J_0(t)dt. \tag{5.9}$$

The amplitudes a_N are the Fourier coefficients in the expansion of $f(\phi)$ and are proportional to Bessel functions

$$a_N = i^N J_N(x).$$

Thus the probability that N pairs have been transferred after the collision is

$$P_N = |a_N|^2 = |J_N(x)|^2.$$

Unfortunately in the heavy ion case x is normally small so that the probability that $|N| > 1$ is very small.

EXTENDED pp-RPA

$$\begin{pmatrix} A_{pp'p''p'''} & B_{pp'h''h'''} \\ B_{p''p'''hh'} & A_{hh'h''h'''} \end{pmatrix} \begin{pmatrix} X_{p''p'''} \\ Y_{h''h'''} \end{pmatrix} = E \begin{pmatrix} X_{pp'} \\ Y_{hh'} \end{pmatrix}$$

E??

PVC

$h_{pp''\lambda\nu}$ =

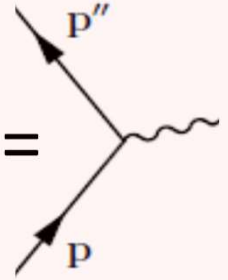

Includes Self-energy and Induced Interaction <-> PVC

$$A_{pp'p''p'''} = [(\epsilon_p + \epsilon_{p'}) + \Sigma_{pp''(p')}(E)\delta_{p'p'''} + \Sigma_{p'p'''(p)}(E)\delta_{pp''} + V^{bare}_{pp'p''p'''} + V^{ind}_{pp'p''p'''}(E) + Exch(p,p')]N_{pp'p''p'''}$$

$$B_{pp'hh'} = [V^{bare}_{pp'hh'} + V^{ind}_{pp'hh'}(E) + Exch(p,p')]\, N_{pp'p''p'''}$$

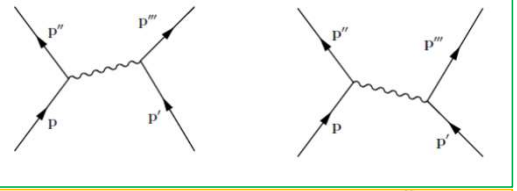

$$V^{ind}_{pp'p''p'''} = \sum_{\lambda\nu}\left[\frac{h_{pp''\lambda\nu}h_{p'''p'\lambda\nu}}{E-(\epsilon^{emp}_{p''}+\epsilon^{emp}_{p'}+\hbar\omega_{\lambda\nu})} + \frac{h_{p''p\lambda\nu}h_{p'p'''\lambda\nu}}{E-(\epsilon^{emp}_{p}+\epsilon^{emp}_{p'''}+\hbar\omega_{\lambda\nu})}\right]$$

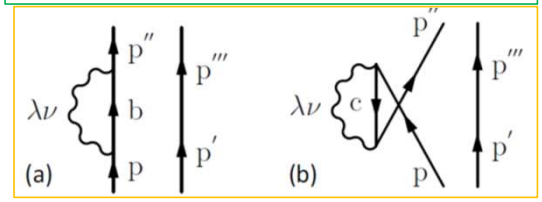

$$\Sigma_{pp''(p')}(E) = \sum_{b,\epsilon_b>\epsilon_F\lambda\nu}\frac{h_{pb\lambda\nu}h_{p''b\lambda\nu}}{E-(\epsilon^{emp}_{b}+\epsilon^{emp}_{p'}+\hbar\omega_{\lambda\nu})} + \sum_{c,\epsilon_c<\epsilon_F\lambda\nu}\frac{h_{pc\lambda\nu}h_{p''c\lambda\nu}}{E-\epsilon^{emp}_{c}-\epsilon^{emp}_{p'}+\hbar\omega_{\lambda\nu}} \quad (6)$$

EXTENDED pp-RPA

The energy dependence of Self-energy and Vind
"hiddes" the amplitudes on the intermediate states:

HIDDEN AMPLITUDES

$$X_{pp'\nu} = \sum_{p''} X_{pp''} \frac{h_{p''p'\nu}}{E - (\varepsilon_p + \varepsilon_{p'} + \hbar\omega_\nu)} + \sum_{p''} X_{p''p'} \frac{h_{p''p\nu}\,(-)^{j_p - j_{p'} - \lambda}}{E - (\varepsilon_p + \varepsilon_{p'} + \hbar\omega_\nu)}$$

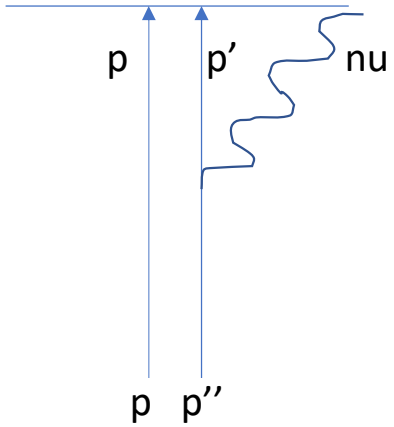

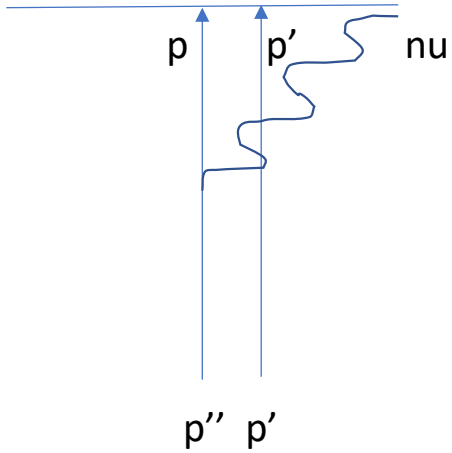

1. Nuclear Superfluidity: Inertial Mass in Exotic Decay (14C, 24Ne,..

(internal 2-nucleon transfer steps: hopping model)

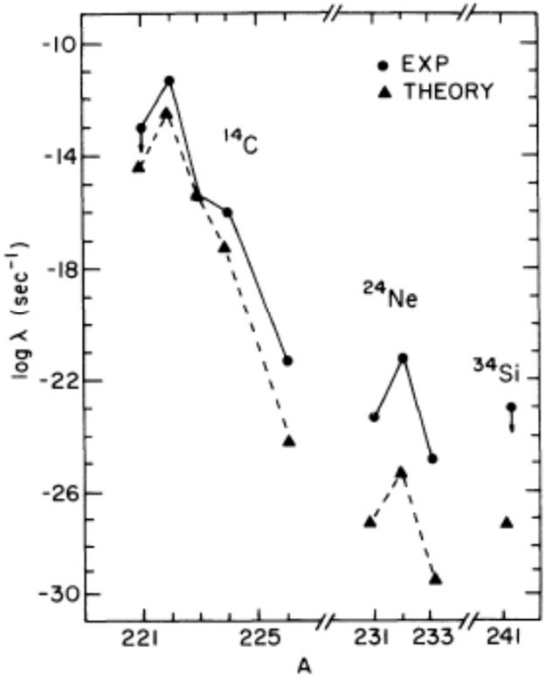

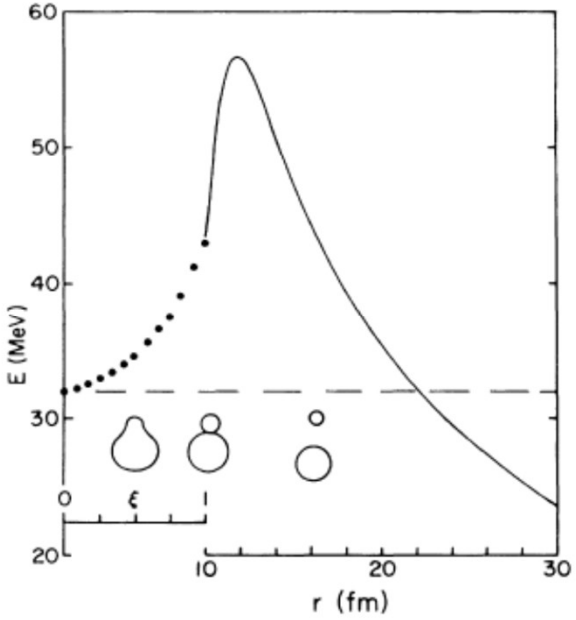

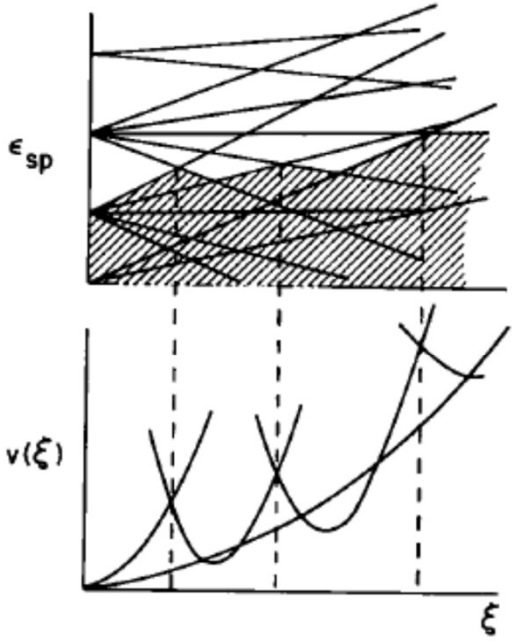

$$\left(-\frac{\hbar^2}{2D}\frac{d^2\Phi(\xi)}{d\xi^2}+V(\xi)\right)\Phi_\alpha(\xi)=E\Phi_\alpha(\xi)\,.$$

$$D=\hbar^2\frac{2G}{\Delta_\nu^2+\Delta_\pi^2}\left(\frac{dn}{d\xi}\right)^2.$$

Barranco et al. PRL60, 507 and Nucl.Phys.A 512 (1990)253

Physics — VIEWPOINT

The Tiniest Superfluid Circuit in Nature

A new analysis of heavy-ion collision experiments uncovers evidence that two colliding nuclei behave like a Josephson junction—a device in which Cooper pairs tunnel through a barrier between two superfluids.

By Piotr Magierski

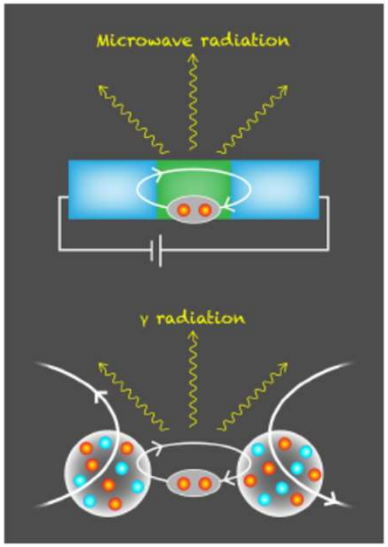

2. Josephson Junctions (DC and AC): In Condensed Matter

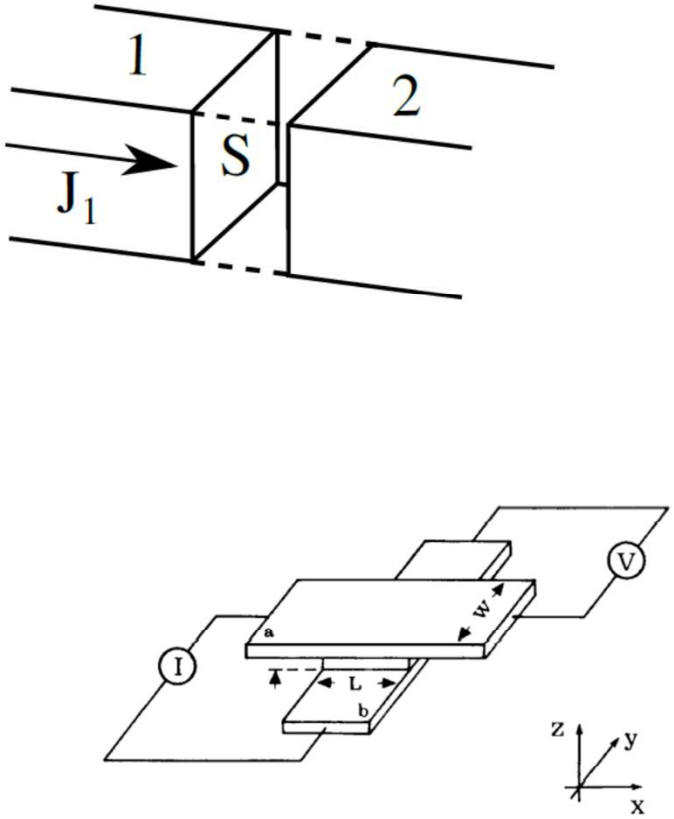

Figure 1.1 Tunneling junction of cross-type geometry. The dimensions are L and W; *a* and *b* are the two superconducting films.

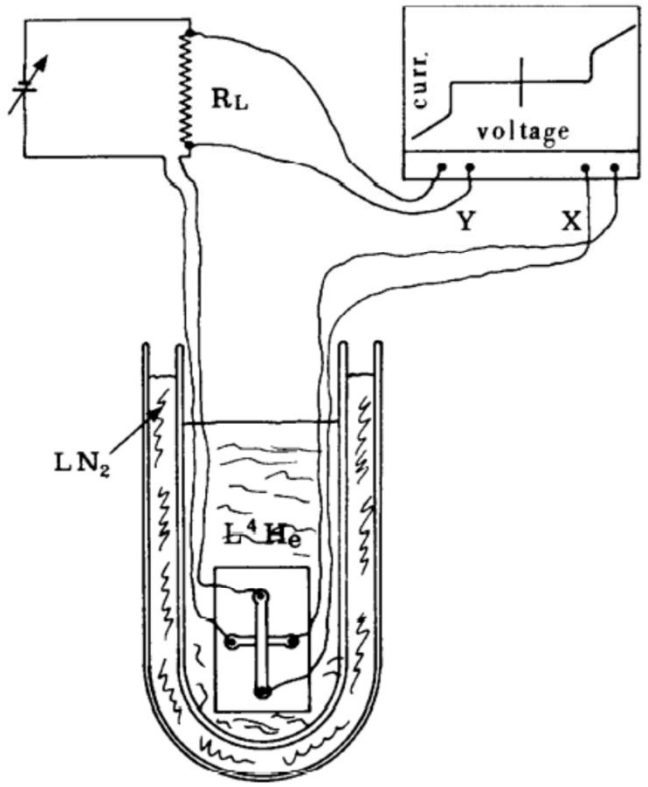

Figure 3.9 Schematic of the experimental apparatus used to measure the voltage-current characteristics of a junction. The inner dewar in which the sample is inserted is filled with liquid helium (L^4He), the outer dewar contains liquid nitrogen (LN_2).

$$a(=b+2)+A \rightarrow f(=b+1)+F(=A+1) \rightarrow b+B(=A+2) \tag{116}$$

Making use of the notation $\alpha \equiv (a, A), \gamma \equiv (f, F)$ and $\beta \equiv (b + B)$. one can write the successive transfer amplitude in the semiclassical approximation ([51] p. 306 Eq. (23)), as

$$(a_\beta(t))_{succ} = \left(\frac{1}{i\hbar}\right)^2 \sum_{\gamma\neq\beta} \int_{-\infty}^{t} dt' \, \langle \Psi_\beta | V_\beta - \langle V_\beta \rangle | \Psi_\gamma \rangle_{\mathbf{R}_{\beta,\gamma}(t')}$$
$$\times \int_{-\infty}^{t'} dt'' \, \langle \Psi_\gamma | V_\alpha - \langle V_\alpha \rangle | \Psi_\alpha \rangle_{\mathbf{R}_{\gamma,\alpha}(t'')}, \tag{117}$$

where the quantal *cm* coordinate $\mathbf{r}_{\beta\gamma} = (\mathbf{r}_\beta + \mathbf{r}_\gamma)/2$ should be identified with the average classical coordinate, i.e. $\mathbf{r}_{\beta\gamma} \rightarrow \mathbf{R}_{\beta\gamma} = (\mathbf{R}_\beta + \mathbf{R}_\gamma)/2$ which, together with $\mathbf{v}_\beta = \dot{\mathbf{R}}_\beta$ and similar for the channel γ, are assumed to describe the motion of the centers of the wavepackets, and satisfy the classical equations $m_\beta \dot{\mathbf{v}}_\beta = -\boldsymbol{\nabla}_\beta U(\mathbf{R}_\beta)$. The functions Ψ describe the structure of the nuclei and, e.g. $\Psi_\alpha = e^{-i\frac{E_\alpha}{\hbar}t}\psi_\alpha$ while $\psi_\alpha = \psi^a(\xi_a)\psi^A(\xi_A)$ is the product of the intrinsic BCS wavefunctions describing the structure of nuclei a and A, ξ being the corresponding intrinsic variables. One can rewrite (117) as,

$$(a_\beta(t))_{succ} = \left(\frac{1}{i\hbar}\right)^2 \sum_{\gamma\neq\beta} \int_{-\infty}^{t} dt' \, \langle \Psi_\beta | V_\beta - \langle V_\beta \rangle | \psi_\gamma \rangle_{\mathbf{R}_{\beta,\gamma}(t')}$$
$$\times \int_{-\infty}^{t'} dt'' \, \langle \psi_\gamma | V_\alpha - \langle V_\alpha \rangle | \Psi_\alpha \rangle_{\mathbf{R}_{\gamma,\alpha}(t'')} e^{i\frac{E_\gamma}{\hbar}(t''-t')}, \tag{118}$$

Assuming the quasiparticle excitation energies E_γ to be much larger than the reaction $Q-$value, the periodic functions in (119) oscillate so rapidly, that the outcome of the integration in (117) amounts to nothing unless $t' \approx t''$. In other words and further assuming that the matrix elements (formfactors) are smooth functions of time along the trajectories of relative motion one can write $\sum_{\gamma\neq\beta} \exp\left(i\frac{E_\gamma}{\hbar}(t''-t')\right) \approx \frac{1}{\Delta E}\int dE \exp\left(i\frac{E}{\hbar}(t''-t')\right) \approx \frac{\hbar}{\Delta E} \times \delta(t''-t')$, where $1/\Delta E$ is the average density of levels of the two-quasiparticle states. Making use of Eq. (9), one can write Eq. (118) as,

$$(a_\beta(t))_{succ} = \left(\frac{1}{i\hbar}\right)^2 \int_{-\infty}^{t} dt' \langle \psi_\beta | (V_\beta - \langle V_\beta \rangle) | \psi_\gamma \rangle_{\mathbf{R}_{\beta,\gamma}(t')}$$
$$\times \frac{\hbar}{\Delta E} \, {}_{\mathbf{R}_{\gamma,\alpha}(t')} \langle \psi_\gamma | V_\alpha - \langle V_\alpha \rangle | \psi_\alpha \rangle \, e^{i\frac{Q_{2n}}{\hbar}t'}, \tag{120}$$

4. The Legnaro's 116Sn+60Ni 2NT and 1NT: BCS ground states and quasiparticles

	ϵ_{l_j}	E_{l_j}	$V^2_{l_j}$	B_{l_j}	E_{l_j}	$V^2_{l_j}$	B_{l_j}
$2d_{5/2}$	-11.51	2.35	0.874	0.658	2.35	0.874	0.575
$1g_{7/2}$	-10.86	1.92	0.790	0.910	1.92	0.789	0.816
$3s_{1/2}$	-9.70	1.56	0.487	0.483	1.57	0.484	0.500
$2d_{3/2}$	-9.51	1.58	0.428	0.661	1.58	0.424	0.699
$1h_{11/2}$	-8.12	2.25	0.140	0.770	2.26	0.139	0.847

Table 1: Properties of the five valence states calculated in ^{115}Sn, starting from the single-particle energies ϵ_{l_j} shown in [1]. The quasiparticle energies E_{l_j}, the occupation probabilities $V^2_{l_j}$ and the transfer spectroscopic amplitudes B_{l_j} shown in Table 1 of ref. [1] are shown in the second, third and fourth column. They are compared in the last three columns with the corresponding quantities recalculated here with a pairing coupling constant $G = 0.217$ MeV (25/A).

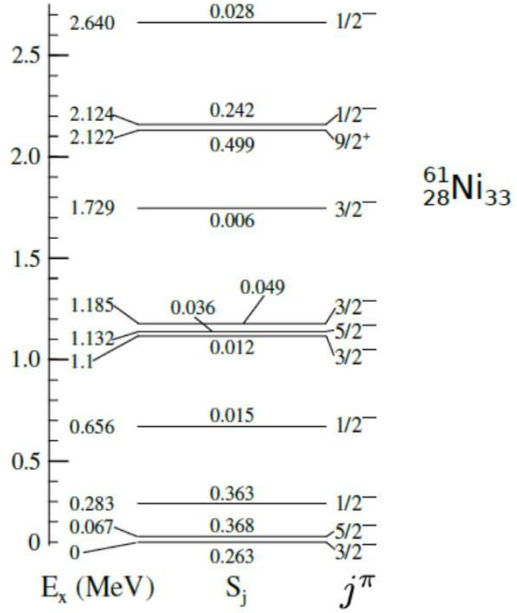

	ϵ_{l_j}	E_{l_j}	$U^2_{l_j}$	B_{l_j}	B_{l_j}
$2p_{3/2}$	-11.33	1.56	0.33	0.524	0.665
$2p_{1/2}$	-9.66	1.83	0.65	0.500	0.477
$1f_{5/2}$	-9.33	2.05	0.400	0.34	0.849
$1g_{9/2}$	-5.16	5.80	0.500	0.1	1.224

Table 2: Properties of the four valence states calculated in ^{61}Ni, starting from the single-particle energies ϵ_{l_j} shown in [1]. The quasiparticle energies E_{l_j}, the occupation probabilities $U^2_{l_j}$ and the transfer spectroscopic amplitudes B_{l_j} shown in Table 1 of ref. [1] are shown in the second, third and fourth column. The values of the spectroscopic are compared in the last column with the value obtained from the relation $B = UV\sqrt{j+1/2}$, using $V^2 = 1 - U^2$.

A new set of calculations was carried out, using slightly modified inputs.

nl_j	ϵ_{nl_j} (MeV)	E_{nl_j} (MeV)	$U^2_{nl_j}$
$2p_{3/2}$	-7.82	1.05	0.44
$2p_{1/2}$	-6.26	1.76	0.90
$1f_{5/2}$	-7.04	1.22	0.24
$1g_{9/2}$	-3.30	4.51	0.99

Table 3: Quasiparticle energies and amplitudes obtained in a BCS calculation for ^{60}Ni with a pairing constant $G = 0.331$ MeV ($= 19.9/A$), following ref. [6].

6. Velocity of the Transfered (nuclear) Cooper Pair.

6.2 Simulated data (DWBA calc's) as a function of pairing interaction.

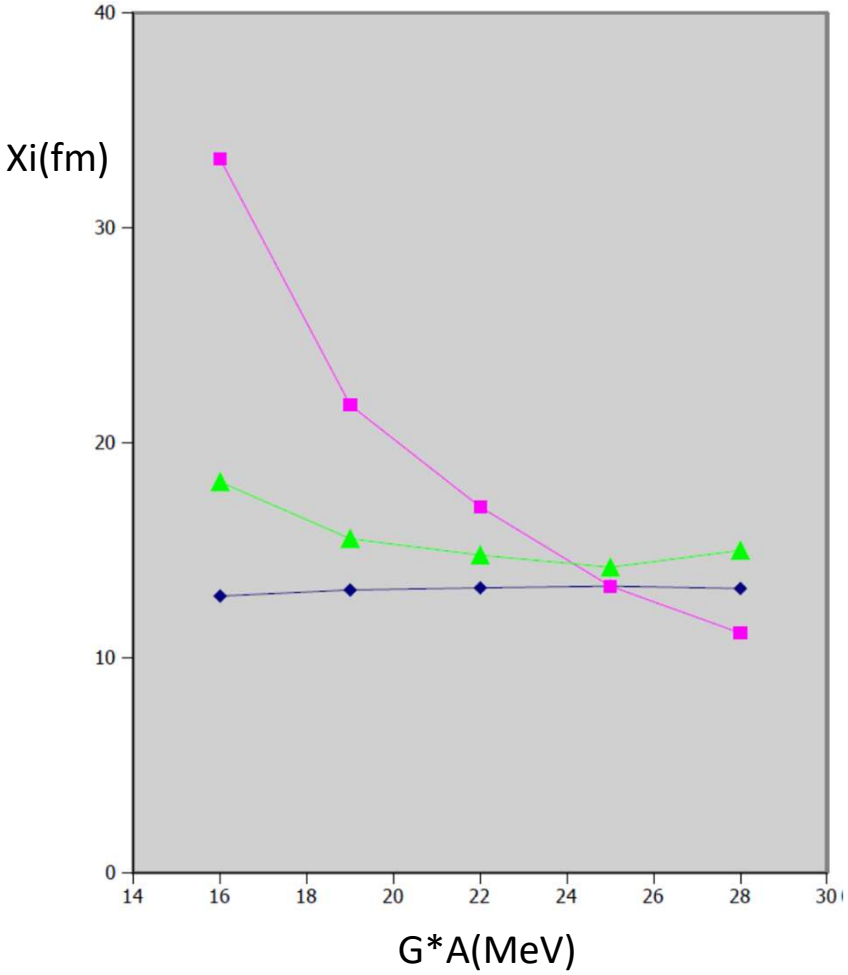

$$\frac{(D_0)_c - (R(^A) + R(^b) + a)}{\tau_{coll}} = \frac{1}{m}\frac{\hbar}{\xi}$$

Some de-pairing velocity effect seems to be present in DWBA

4. The Legnaro's 116Sn+60Ni 2NT and 1NT data at different E_cm:

4.1 Semiclassical analysis.

In heavy ion collisions below the Coulomb barrier with typical values of the ratio $D_0/\lambda\!\!\!^{-} \approx 10^2$ between the distance of closest approach and the reduced de Broglie wavelength, Cooper pair tunneling can be described in terms of the semiclassical second order transfer amplitude (see [51] p. 306 Eq. (23)),

$$(a_\beta)_{succ} \approx \left(\frac{1}{i\hbar}\right)^2 \times \sum_{Ff \neq Bb} \int_{-\infty}^{\infty} dt \, \langle \Psi_{Bb} | V_{Ff} - \langle V_{Ff} \rangle | \Psi_{Ff} \rangle_{\mathbf{R}_{Bb,Ff}(t)} \, e^{i\frac{(E_{Bb}-E_{Ff})}{\hbar}t} \times \int_{-\infty}^{t} dt' \, \langle \Psi_{Ff} | V_{Aa} - \langle V_{Aa} \rangle | \Psi_{Aa} \rangle_{\mathbf{R}_{Aa,Ff}(t')} \, e^{i\frac{(E_{Ff}-E_{Aa})}{\hbar}t'}.$$

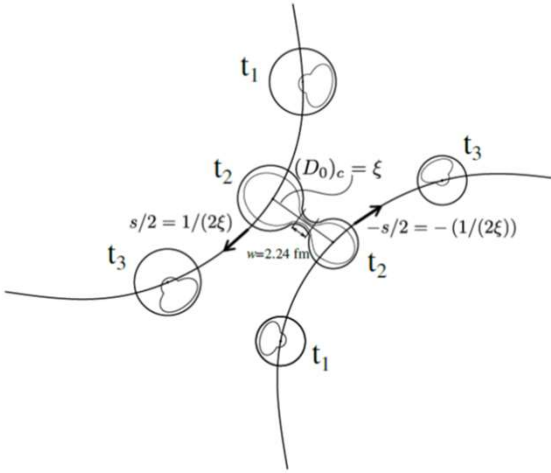

$B_j = \sqrt{\frac{(2j+1)}{2}}\, U'_j V'_j,$